Under the cover of darkness: how clubroot disease affects *Arabidopsis thaliana* physiology during the night.

Andrea Garvetto[1], Susann Auer[2], Freia Benade[2], Michaela Hittorf[1], Jutta Ludwig-Müller[2], Sigrid Neuhauser[1]

Corresponding authors: Andrea Garvetto (andrea.garvetto@uibk.ac.at), Sigrid Neuhauser (sigrid.neuhauser@uibk.ac.at)

Abstract

Background: *Plasmodiophora brassicae* (Phytomyxea, Rhizaria) is the etiological agent of clubroot disease, one of the most important diseases of Brassicaceae crops. Alteration of metabolism and hormone homeostasis leads to the formation of tumor-like galls in the root system of affected plants. Host plant energy metabolism and developmental processes are under strong temporal control exhibiting differences between day and night. The very same processes are affected by clubroot, but the effect of the infection on the host plant in the night has never been investigated. This study uses time-resolved transcriptome analyses to explore how *P. brassicae* affects *A. thaliana* in the night during intermediate (14 DAI) and late (21 DAI) infection.

Results: Day-night differences in gene expression were more pronounced in younger rather than older plants in our differential gene expression (DGE) analysis, regardless of infection status. Consequently, intermediate phases of infection showed more day-night differences than later ones. Clustering of differentially expressed genes (DEGs) in functional categories highlighted how some of the typical processes known to be disrupted by clubroot infection are more significantly affected in the night and also uncovered some disrupted exclusively in the night. Among these, RNA modification stood out as the most unambiguously highly upregulated process in infected *Arabidopsis* roots in the night. Analysis of the interaction between clubroot infection and diel oscillations in gene expression also showed a higher interplay between clubroot and time in younger plants, where many genes lost their normal day/night oscillations during the infection. Interestingly, few genes central to the plant circadian clock were found to be affected and lost their normal rhythmicity with the infection.

Conclusions: *P. brassicae* induces night time specific changes in gene expression during the metabolically active phases of the infection. In addition, the infection does affect rhythmic gene expression in plants including core genes of the circadian clock. Time-resolved datasets could help to better understand the interaction between *P. brassicae* and its hosts and constitute the first step for the investigation of clubroot-induced changes in rhythmic gene expression.

Keywords: Biotrophic parasite, Circadian, Host-pathogen interactions, *Plasmodiophora brassicae,* Protist, Time-resolved transcriptome

Background

Responsible for around 10 % of harvest losses worldwide, *Plasmodiophora brassicae* Woronin is one of the most impactful pathogens of Brassicaceae crops [1]. This obligate biotrophic parasitic protist belonging to the class Phytomyxea (Rhizaria; [2]) has a complex life cycle featuring a short-lasting, symptomless primary phase occurring in the root hairs and epidermis of a broad array of plant hosts; and a secondary, long-lasting and symptomatic phase, specifically occurring in hosts within the family Brassicaceae where durable resting spores are formed [3], [4]. The secondary phase of the infection occurs in the root cortex and stele, where it impacts the host physiology and anatomy, causing successive hyperplasia and hypertrophy in the affected tissues [5], leading to the typical gall formation from which the common name "clubroot disease" derives. This modification of the host anatomy and physiology is required for the parasite to generate a strong local nutrient sink at the site of infection, inducing a systemic redirection of the host photosynthates [6]. Clubroot impact on susceptible plants is heavy, with infected hosts featuring stunted growth, increased susceptibility to wilting and early onset of senescence [7]. Molecular investigations have been proven paramount in understanding the influence of *P. brassicae* on its host physiology [8]–[11], highlighting highly impacted processes deserving more extensive investigation, such as: cell wall expansion, remodelling and lignification [12], [13]; cell cycle activation and modification [5] and sugar homeostasis [14]. Pathogen-induced disruption of sugar homeostasis is crucial to the trophic interaction between *P. brassicae* and its host, whereby the parasite generates a sugar sink in the gall tissue by increasing symplastic sugar delivery via extracellular invertases [14] and by promoting phloem differentiation and local accumulation of sugar transporters at the site of infection [15].

Because of its central role in plant physiology, the disruption of sugar metabolism likely mediates systemic reactions at the organism level in clubroot disease, but the substantial anatomical changes observed are also the result of its impact on hormone homeostasis [16], [17]. Hormones involved in plant defence such as salicylic acid (SA) and jasmonic acid (JA) have been broadly linked to heightened resistance against *P.*

59 *brassicae* [18]–[21]; and the parasite seems to directly disrupt both [22], [23]. *P. brassicae* also induces
60 accumulation of the stress-related hormone abscisic acid (ABA) as a consequence of the impaired vascular
61 transport and water supply caused by gall formation [16]. *Arabidopsis* mutants impaired in the perception
62 of the stress-related hormone ethylene (ET) showed increased resistance only when the mutation targeted
63 the crosstalk between ethylene and auxin transport [16], [24]. Indeed, auxins have been found to play an
64 important role in clubroot disease, gradually increasing in the galls with the development of the infection
65 and mutants impaired in indole acetic acid (IAA) biosynthesis were found to produce smaller or
66 developmentally delayed galls [25], [26]. Investigations highlighted how the *P. brassicae* protein PbGH3
67 can conjugate auxins [23] and the recently identified gene *SYNERGISTIC ON AUXIN AND CYTOKININ 1*
68 (*SYAC1*), a cross-talk component between the auxin and cytokinin pathways in *A. thaliana* roots, made
69 plants more susceptible to infection and exacerbated the symptoms of clubroot when constitutively
70 expressed; supporting a pivotal role of the auxin-cytokinin balance in this interaction [27]. In biotrophic
71 interactions between plants and pathogens, the role of cytokinins in establishing local nutrient sinks and
72 in suppressing cell death has long been recognized [28], nonetheless the overall impact of *P. brassicae* on
73 host cytokinins is ambiguous. Studies have reported both suppression and increase in metabolism and
74 levels of cytokinins [29]–[31], but decreased cytokinin degradation on the host side [8] coupled with
75 evidence of endogenous cytokinin production by the pathogen [32], [33] seem to support the need for
76 cytokinins in the local establishment of a *de novo* meristematic sink area in the initial phases of infection
77 [17], [34].

78 The above listed processes impacted by *P. brassicae* are known to be strongly influenced by diel (i.e., day
79 and night) and circadian oscillations in plants. While most living organisms have evolved a way to
80 synchronise their physiology to the environmental rhythms in order to maximize their fitness, plants are
81 particularly affected by these rhythms as they rely for growth and development on light, arguably one of
82 the most rhythmic timers/*zeitgebers* on the planet [35], [36]. Changes in light and other oscillating

83 environmental parameters such as temperature, entrain the core circadian clock, a
84 transcriptional/translational feedback loop central to the adjustment of rhythmic physiological responses
85 in plants [37]. Moreover, the same rhythmic physiological processes influenced by environmental factors
86 via the circadian clock also act back on it as endogenous *zeitgebers* such as in the case of sugars derived
87 from photosynthetic carbon fixation, whose correlation with the availability of diurnal light has long been
88 ascertained [38], [39].

89 Besides being under strong temporal control, the availability of photosynthates is also spatially resolved.
90 For example, a sucrose transporter involved in phloem unloading has been found to be specifically
91 upregulated in roots during the night, matching a steady increase in nocturnal root growth that peaks
92 shortly after dawn [40]–[42]. The synthesis and accumulation of defence hormones has also been reported
93 to be under the influence of diel oscillations in gene expression, in particular the synthesis and
94 accumulation of competing JA and SA; with JA-mediated resistance to herbivores and necrotrophic
95 pathogens being upregulated in the day, whilst SA-mediated resistance to biotrophic parasites heightened
96 in the night [43]. As already mentioned, the majority of the processes under circadian control also provide
97 retroactive feedback to inform and entrain the circadian clock itself [37]. Since pathogens are known to
98 manipulate hormones and to strongly affect energy homeostasis, it is possible that these processes are
99 central to mediate pathogen-induced modifications on the host internal clock [44].

100 As an obligate biotrophic intracellular parasite, *P. brassicae* is likely to have evolved ways to influence the
101 rhythmic gene expression of its host in order to maximize its benefits and hinder defence; but until now
102 only the diurnal phase of clubroot infection has been explored. This study provides the first time-resolved
103 RNA-seq dataset, covering both day and night, for intermediate (14 days post-inoculation) and mature (21
104 days post-inoculation) clubroot disease in *Arabidopsis thaliana.* Our exploration of the data generated was
105 used to uncover physiological processes of the host that are influenced by the parasite specifically during

the night and further to understand the interplay between diurnal/nocturnal changes in gene expression and clubroot disease.

Methods

Experimental setup & biological material

After germination, seedlings of *Arabidopsis thaliana* ecotype Col-0 obtained from the Seed Stock Centre (stock N1092, Nottingham, UK) were grown on a soil substrate (Einheitserde Type P, pH 5.8; Hermina Samen, Germany) mixed with sand (Sahara Spielsand; Hornbach Germany) in the ratio 4:1. This soil mixture was steam-sterilized prior to use for 120 minutes at 100 °C. All plants were grown in a Sanyo MLR-350H climate chamber at a temperature of 23°C during the day and 18°C during the night. The light/dark cycle was set to 12:12 hours, with a light intensity of 100 µmol. Genome-sequenced *Plasmodiophora brassicae* isolate e3 [45] obtained from Dr. Siemens [46] was propagated on *B. rapa* var. *pekinensis* (ISP International Seed Processing GmbH, Quedlinburg, Germany) and pure spore suspensions were obtained as described in [23]. One week after germination, *A. thaliana* Col-0 plants were inoculated with 1 mL of *P. brassicae* isolate e3 spore suspension at a concentration of 10^6 spores/mL in 50 mM KH_2PO_4 buffer (pH 5.5, adjusted with K_2HPO_4) or with a mock inoculation of an equal amount of the same buffer. Healthy and infected plants were harvested 14 and 21 days after inoculation (DAI), in each occasion at four different time points: two points during the “day” (5 hr 50’ and 10 hr 40’ after artificial dawn) and two points during the “night” (15 hr 30’ and 19 hr 20’; i.e., 3 hr 30’ and 7 hr 20’ after artificial dusk). Eight to twelve plants were grown per each time point / treatment and harvested by pooling four plants in 1 mL ice-cold RNAlater (Ambion, Austin, TX, USA) in 1.5 mL Eppendorf tubes. Samples were then left to rest overnight, before removing and refreshing the RNAlater and storing them at -80°C until RNA extraction.

RNA extraction & sequencing

129 Samples in RNAlater were thawed on ice and one or two plants (when biomass from a single plant
130 specimen was judged insufficient for RNA extraction) per each tube were transferred to ethanol-sterilised
131 and RNAseAway treated tin foil squares with equally treated steel tweezers. Plants were carefully wrapped
132 and snap-frozen in liquid nitrogen before transferring them in pre-mixed bead matrix tubes (D1034-MX;
133 Biozym, Hessisch Oldendorf, Germany) amended with 200 µL IB buffer (SPLIT RNA Extraction Kit, Lexogen,
134 Vienna, Austria) to decrease the risk of RNA degradation and immediately homogenized with a FastPrep
135 bead mill (MP Biomedicals, Santa Ana, CA, USA) for 40 s at 60 ms^{-1} three times. After tissue disruption,
136 another 200 µL of ice cold IB buffer was added to the samples. The RNA extraction proceeded following
137 the protocol SPLIT RNA extraction of total RNA (SPLIT RNA Extraction Kit, Lexogen, Vienna, Austria) as
138 suggested by the manufacturer without further modifications. Assessment of the RNA extracts quality and
139 quantity was performed on an Agilent Bioanalyzer 2100 (Agilent Technologies, Palo Alto, CA, USA) and
140 Quantus fluorometer (Promega Corporation, Fitchburg, WI, USA). Strand-specific library preparation was
141 performed on poly-A-selected mRNA using a NEBNext Ultra II Directional RNA Library Prep Kit with
142 NEBNext Poly(A) mRNA Magnetic Isolation Module and NEBNext Multiplex Oligos for Illumina (New
143 England Biolabs, Ipswich, MA, USA). The quality and concentration of cDNA in the resulting libraries was
144 assessed on an Agilent Bioanalyzer 2100 and Quantus fluorometer, before paired-end sequencing (2x150
145 bp on a NovaSeq S1; Illumina, San Diego, CA, USA) at the VBCF NGS Unit (Vienna, Austria).

146 *Sequencing data processing*

147 Read quality was checked using FastQC [47] and quality reports visualized in MultiQC v1.6 [48] before and
148 after read filtering and adapter trimming with Trim Galore v0.6.2 (quality score threshold 30;
149 https://zenodo.org/doi/10.5281/zenodo.5127898). To assign reads to the host plant and the parasite,
150 Bowtie2 v2.3.5.1 [49] was used to map them against the concatenated genomes of *Arabidopsis thaliana*
151 (TAIR10; [50]) and *Plasmodiophora brassicae* (Pldbra_eH_r1) with a "Place-to-go-based" approach as
152 defined in [51]. Obtained read pools (separately for the host and the parasite) were assembled with Trinity

153 v2.10.0 (in genome guided mode; [52]) and resulting transcripts annotated with Trinotate v3.2.1 [53].
154 Expression estimates were obtained by pre-aligning the reads to the transcripts using STAR v2.7.1a [54]
155 and assigned to assembled transcript with Salmon [55]. Raw NGS sequences of the dataset obtained in
156 this study are deposited in NCBI Sequence Read Archive (SRA) under the BioProject accession number
157 PRJNA1212907.

158 *Differential gene expression*

159 DESeq2 Bioconductor package [56] in R [57] was used to estimate differential gene expression. In order to
160 detect differences in the response of plants to infection by *P. brassicae* during the day and during the night
161 differentially expressed genes (DEGs) were calculated by pooling counts from all time points sampled
162 during the day (i.e., 5 hr 50' and 10 hr 40' after artificial dawn) and during the night (15 hr 30' and 19 hr
163 20' after artificial dawn).

164 This resulted in six replicates for each of the four conditions, as defined by the two factors "Condition"
165 (Infected or Control) and "Time point" (Day or Night; Additional file 1). An experimental design with two
166 factors and interaction was used for estimating the DEGs, thus resulting in five comparisons: infected vs
167 control in the day, infected vs control in the night, control in the night vs in the day, infected in the night
168 vs in the day and interaction. Genes were considered differentially expressed when the adjusted p-value
169 was ≤ 0.05 (Wald test p-value adjusted for multiple testing with Benjamini–Hochberg correction) and a
170 $\log_2$-fold change was ≤ -1 or ≥ 1.

171 *Principal component analysis and Venn diagram*

172 Principal component analysis (PCA) was calculated in the DESeq2 Bioconductor package in R [56] and
173 further modified in ggplot2 [58]. The PCA was performed on variance stabilizing transformed (vst) count
174 data from the DESeqDataSet object, without taking into account the sample information (i.e., blind=TRUE),

175 as suggested by the DESeq2 manual. Venn diagrams on DEGs were calculated in R with the Package
176 VennDiagram [59].

177 *GO term over representation analyses*

178 ClusterProfiler [60] was used within R to perform gene ontology (GO) over-representation tests using lists
179 of DEGs in the comparisons between infected and healthy plants in the day and in the night. Significance
180 of the enriched GO categories was assessed by Fisher's exact test controlled for False discovery rate (FDR)
181 with Benjamini–Hochberg correction and the q-value cutoff was set to 0.05. Because the RNA-seq strategy
182 adopted was designed to measure all expressed mRNAs (total RNA extraction followed by poly-A tail
183 selection), the background gene list (or "universe") against which over-representation was performed, was
184 composed of a list of all protein coding genes from *A. thaliana* TAIR10 genome release. The package GOplot
185 [61] was used to combine expression data with functional categories. Using the function "circle_dat", the
186 package was used to summarise and append to each enriched GO category an overall expression value
187 (i.e., a z-score) calculated as follows:

188 $$z\ score = \frac{(\text{n° upregulated genes in GO } - \text{n° downregulated genes in GO })}{\sqrt{Total\ n°\ of\ genes\ in\ GO}}$$

189 The function "reduce_overlap" within the same package was used to eliminate all but one GO category
190 sharing more than 25% of the genes before plotting the results with the function "GObubble".

191 *Heatmap of gene expression levels*

192 Genes whose differential expression levels were driven by the interaction between the factor "Time point"
193 and the factor "Condition" were detected and their expression levels were visualised with heatmaps as
194 implemented in the package pheatmap [62] in R, on row-scaled, log-normalised read counts and with
195 default "Euclidean" clustering method. All figures were further refined and finalized in Inkscape [63].

Results

Overview of gene expression levels in infected and healthy plants in the day and in the night

The major factor influencing the clustering of DEGs of *A. thaliana* in PCAs is their response to *P. brassicae* (Fig. 1 A & C). In the intermediate phases of infection (14 DAI) the first two principal components (PCs) explain a cumulative 78% of the variation (Fig. 1 A). Infected and healthy plants strongly separate along the PC1, explaining more than half of the variation in gene expression (63%). Noticeably, the PC2 (explaining 15% of the variation) mostly separated the samples according to night or day (factor "Time point"). Samples collected at 21 DAI seem to be less affected by the time of sampling, with PC1 explaining 83% of the variation and being clearly linked to the infected or healthy status of the plant samples, and PC2 explaining only 5% of the variation (Fig. 1 C) without clear separation of the samples along the factor "Time point". A PCA of the gene expression levels in uninfected plants resulted in a similar pattern, whereby older plants did not show a time-dependent response (Additional File). Befittingly, in plants 14 DAI more than one third (36,75%) of the differentially expressed genes (DEGs) are specific to the night phase and 16,40% to the day (Fig. 1 B), whilst the number of DEGs that are exclusively detected during day or night is decreasing at 21 DAI indicating a reduced influence of the factor "Time point" on gene expression from the intermediate to the late stages of infection (21,48% in the night, 17,52% in the day and 61% shared; Fig. 1 D).

Regulation of enriched GO categories in infected plants during day and night

Differentially expressed genes (DEGs) were predominantly downregulated in infected plants across all sampling times and DAI (Additional File and Additional File). A comprehensive analysis of the average expression within overrepresented GO categories reinforced this trend, revealing a greater proportion of downregulated than upregulated categories. At 14 DAI during the day, 63 GO categories were downregulated, while 25 were upregulated, and one category displayed an equal balance of up- and downregulated genes ("response to molecule of fungal origin"; Fig. 2 A and Table 1).

220 Among the 25 upregulated GO categories in the day, the ten most significantly enriched GO categories
221 (adj. p-value < 0.0003) included “response to toxic substance”, “tetrapyrrole binding”, “anatomical
222 structure formation involved in morphogenesis”, “isoprenoid biosynthetic process”, “regulation of post-
223 embryonic development”, “pigment biosynthetic process”, “signaling receptor activity”, “apoplast”,
224 “plastoglobule” and “photosynthetic electron transport chain”. Conversely, the top ten downregulated GO
225 categories (adj. p-value < 1.95e-7) included “cellular response to hypoxia”, “cellular carbohydrate
226 metabolic process”, “secondary metabolite biosynthetic process”, “NAD+ nucleosidase activity”,
227 “response to salicylic acid”, “programmed cell death”, “positive regulation of response to stimulus”,
228 “benzene-containing compound metabolic process”, “identical protein binding” and “floral organ
229 development” (Fig. 2 B and Table).

230 A similar overall pattern emerged in the night, with 67 downregulated, 30 upregulated and 5 GO categories
231 with a z-score of 0 (Fig. 2 B and Table). The most significantly enriched categories upregulated during the
232 night included “response to toxic substance”, “RNA modification”, “ABC-type transporter activity”,
233 “stomatal closure”, “response to reactive oxygen species”, “defense response to insect”, “regulation of
234 post-embryonic development”, “response to gibberellin”, “recognition of pollen” and “response to
235 extracellular stimulus”. In contrast, categories such as “cellular carbohydrate metabolic process”, “NAD+
236 nucleosidase activity”, “phenylpropanoid metabolic process”, “cellular response to decreased oxygen
237 levels”, “hydrolase activity acting on glycosyl bonds”, “heme binding”, “response to salicylic acid”,
238 “external encapsulating structure organization”, “S-glycoside metabolic process” and “anatomical
239 structure formation involved in morphogenesis” were among the most downregulated.

240 Similar to the observations at 14 DAI, a greater number of downregulated categories compared to
241 upregulated ones is observed at 21 DAI with 94 versus 15 during the day and 79 versus 31 during the
242 night). Notably the total number of affected GO categories is higher, as expected from the higher number
243 of DEGs observed in this phase of infection (Fig. 3, Table and Additional File 4).

244 The 15 overrepresented GO categories during the day are “photosynthesis”, “plastid organization”,
245 “organic acid catabolic process”, “pigment biosynthetic process”, “response to absence of light”,
246 “circadian rhythm”, “response to red or far red light”, “defense response to insect”, “peroxisome”, “Group
247 II intron splicing”, “cell surface receptor signaling pathway”, “triglyceride metabolic process”, “organic
248 cyclic compound catabolic process”, “monosaccharide transmembrane transport” and “inorganic
249 phosphate transmembrane transporter activity”. The ten most significantly enriched categories
250 downregulated in the day are “cellular carbohydrate metabolic process”, “phenylpropanoid metabolic
251 process”, “response to toxic substance”, “NAD+ nucleosidase activity”, “tetrapyrrole binding”, “S-glycoside
252 metabolic process”, “cellular response to decreased oxygen levels”, “response to extracellular stimulus”,
253 “external encapsulating structure organization” and “response to salicylic acid”.

254 In the night several of the ten most enriched GO categories upregulated are shared with the ten most
255 enriched upregulated categories in the day, such as “photosynthesis” and “plastid organization”. Other
256 categories are only related to the ones observed in the day such as “response to light intensity”,
257 “chlorophyll biosynthetic process” and “response to extracellular stimulus”; whilst other specifically
258 upregulated in this phase, as “NAD+ nucleosidase activity”, “response to reactive oxygen species”,
259 “identical protein binding”, “small molecule catabolic process”, and “cellular response to abiotic stimulus”.
260 Equally, among the ten most downregulated categories some share similarities with their day
261 counterparts: “cellular carbohydrate metabolic process”, “external encapsulating structure organization”,
262 “tetrapyrrole binding”, “cellular response to decreased oxygen levels” and “response to salicylic acid”;
263 whilst others are less significantly downregulated: “inorganic ion transmembrane transport”, “terpenoid
264 metabolic process”, “post-embryonic plant morphogenesis” and “ABC-type transporter activity”; or not
265 represented in the day such as: “secondary metabolite biosynthetic process”.

266 *Effect of the interaction between clubroot and time of the day on A. thaliana gene expression*

267 The variables "Condition" and "Time Point" are not fully independent, both influence gene expression at
268 the same time. To identify the genes that are affected by both of these variables we used a statistical
269 "interaction effect" model (IE; [64]). This identified 217 functionally annotated genes at 14 DAI which were
270 strongly impacted by both variables (Fig. 4). These 217 DEGs can be grouped in eight clusters according to
271 their expression patterns. Enriched GO terms could be detected in 6 of these clusters (cluster 1, 3, 4, 5, 6
272 and 8) hinting at how infection and time of the day are affecting processes in the host (Additional File 5
273 GO terms overrepresentation analysis of the clusters of DEGs driven by the interaction between infection
274 and time of the day 14 DAI5).

275 Clusters 1 and 3 are characterised by a loss of diel oscillation in infected plants, where the genes are always
276 active regardless of the time of the day. Cluster 1 is enriched in the terms related to senescence, circadian
277 rhythm and cell signalling, where control plants show upregulation during the day. Cluster 3 is
278 characterised by the terms “response to nitrate” and terms related to the chloroplast membrane, terms
279 showing upregulation in the night in the control. Cluster 7 also loses diel oscillation, but the changes in this
280 cluster are characterised by a downregulation of genes in infected plants which are upregulated during
281 day in control plants.

282 In contrast cluster 2 acquires a diel oscillation in infected plants with genes being upregulated in the day
283 and downregulated in the night, an oscillation absent in the control plants. Genes in cluster 6 show an
284 inversion of the normal pattern of expression, whereby nocturnal upregulation in the control is overridden
285 in infected plants by a nocturnal downregulation (and vice versa). Cluster 6 is enriched in term “response
286 to fructose”. Cluster 4, enriched in terms related to glycosylation of proteins, shows upregulation by the
287 infection with a stronger effect during the day. Clusters 5 and 8 show no distinct pattern. Cluster 5 is
288 associated with the terms “phosphatidylinositol phosphate kinase activity”, “phosphotransferase activity,
289 phosphate group as acceptor” and “nucleoside transmembrane transporter activity” and cluster 8 with
290 terms related to cellular response to abiotic stress and protein localization to the nucleus.

Fewer genes were impacted by the interaction between time of day and infection at 21 days post-infection (DAI) compared to 14 DAI (96 genes with functional annotations). The clustering of the samples cannot discriminate day and night but it maintains a clear separation along infected and control plants (Fig. 5). The pattern of gene expression could divide the DEGs in five clusters, three of which contain enriched GO terms. Genes in cluster 1 and cluster 2 show a general upregulation in infected plants and in cluster 2 terms related to response to hypoxia and sugars were enriched. Cluster 3 shows an opposite pattern, with genes mainly downregulated by the infection enriching categories related to the development of anatomical structures and cytoplasmic stress granules. The main expression pattern identified in cluster 4 is the upregulation of genes normally downregulated during the night. This cluster is described by GO terms related to circadian/rhythmic processes, chloroplast membranes, histone methylation and transport of organic acids. Cluster 5 shows a more complex expression pattern, were most of the genes upregulated in the night in control conditions are upregulated in the night in infected conditions and vice versa, but no enriched GO terms were found for this cluster.

Discussion

This study explores the effects of *P. brassicae* infection on diel oscillations in *A. thaliana*, identifying significant effects on gene expression dynamics. Intermediate infection stages (14 DAI) show strong diel influence, aligning with peak metabolic activity of the parasite and initiation of gall formation [3], [34], whereas later stages (21 DAI) reveal reduced rhythmicity, likely driven by plant senescence rather than the pathogen. Nonetheless, overall the strongest driver of gene expression changes is the infection itself, overriding time-of-day effects, and highlighting a complex interaction between host circadian mechanisms and pathogen strategies. Processes such as phenylpropanoid metabolism and RNA modification are disproportionately affected at night and we link these to disruptions in starch accumulation and defenses in infected roots.

314 Time-resolved RNA-seq analysis of clubroot disease in *A. thaliana* shows an increasing number of DEGs as
315 the infection advances, reflecting the progressive cell-by-cell colonisation of roots by *P. brassicae* [65] and
316 its systemic and diversified impact on the plant, where each cell in infected tissues may contain parasitic
317 plasmodia at different stages of development. Existing transcriptomic datasets featuring a developmental
318 dimension support this [10], [66]. The effect of diel changes in gene expression in infected plants appear
319 to be stronger at 14 DAI as compared to 21 DAI (Fig.1) and a decreased influence of day and night on gene
320 expression is also evident in control plants (Additional File 2) indicating a general circadian dampening
321 with plant age. The relationship between senescence and circadian rhythm in ageing plants has been
322 studied in leaves, revealing a similar pattern of reduced amplitude and an increase in frequency of
323 circadian oscillations with age [67]–[69]. A specific circadian clock or 'root clock' has been shown to
324 integrate exogenous cues such as light, water availability and temperature in order to adjust root gene
325 oscillations with the external environment [70]. The root clock is closely linked to shoot apical meristem
326 circadian oscillations [71]–[73] and likely influenced by senescence in above ground tissues, although
327 specific work on the root developmental clock has not yet addressed its interplay with root senescence
328 itself [74]. At 21 DAI clubroot infected *A. thaliana* plants are four weeks old and therefore approaching the
329 end of their six week life-cycle [75]. This advanced senescence would explain the reduced influence of diel
330 rhythmicity observed at 21 DAI (Fig. 1 C&D, 3 and 5). In contrast, a clear influence of night and day has
331 been observed at 14 DAI (14 DAI; Fig. 1 A&B, 2 and 4).

332 The infection is the strongest driver of changes in gene expression (Fig. 1 A), but the genes affected differ
333 between day and night especially in the intermediate phases (i.e., 14 DAI; Fig. 2 and 3; Tables 1 and 2). GO
334 categories enriched by infection-related DEGs during the day are in line with previous, comparable studies
335 [10], [11]. Nonetheless, interpreting these results requires careful consideration, since each enriched GO
336 category contains upregulated and downregulated genes and since the z-score reflects only the count of
337 genes up/downregulated but not the magnitude of changes. For example, specific genes involved in low

338 oxygen responses during clubroot such as PYRUVATE DECARBOXYLASE 1 (PDC1) and ALCOHOL
339 DEHYDROGENASE 1 (ADH1) have been found to be upregulated in previous studies [76]. These specific
340 genes are also upregulated in our dataset, even though low oxygen response categories are overall
341 downregulated, seemingly contradicting earlier findings (Fig. 2). Similarly, cell wall-related categories are
342 consistently downregulated in our dataset, though individual genes like expansins and pectin
343 methylesterases show contrasting gene-specific expression patterns, which is in line with previous findings
344 [10]–[12].

345 Occasionally, genes known to be affected by clubroot disease are more severely impacted in the night such
346 as in the case of the downregulation of "phenylpropanoid metabolic process" 14 DAI (64 genes enriching
347 the category in the night as compared to 49 in the day; Additional File 7). Phenylpropanoids are known to
348 be involved in plant mechanical and chemical defence, especially via the induction of lignin deposition in
349 secondary cell walls and the accumulation of flavonoids [77]. The pivotal importance of lignification of
350 secondary cell walls in preventing the colonization and spread *P. brassicae* is known, with *P. brassicae*
351 infection actively interfering in this process in susceptible *B. napus* varieties [13]. Downregulation of lignin
352 biosynthesis has been observed in clubroot infected *A. thaliana* [9]. It is therefore interesting to notice
353 that the deregulation of phenylpropanoid biosynthetic processes, and putatively lignin deposition, seems
354 to be more intense during the night.

355 The GO category "RNA modification" was the most striking night-exclusive GO category in terms of
356 differential expression, gene counts and significance. The majority of genes (90/101) are assigned to
357 pentatricopeptide repeat-containing proteins (PPR proteins), with most of them being upregulated
358 (86/101). Land plant genomes harbour an expanded number of PPR protein encoding genes [78], and
359 many of them are involved in the RNA stabilisation, splicing and editing in chloroplasts and mitochondria
360 and are necessary for the correct development and functioning of the target organelle [78], [79]. The
361 upregulation of genes potentially involved in chloroplast biology in the root of *A. thaliana* infected with

362 clubroot might seem counterintuitive, but it is important to remember that amyloplasts are plastid-
363 derived storage organelles for starch accumulation. The increase of amyloplasts in the root cortex of plants
364 affected by clubroot is a well-known and documented phenomenon [80], [81]. Disruption of transcription
365 has been shown to inhibit the differentiation of proplastids into amyloplasts [82], [83], suggesting a
366 potential involvement of PPR-mediated post-transcriptional editing in the transition. Cytokinins are
367 another factor necessary for the transition from proplastid to amyloplast in cell cultures [83]. Cytokinins
368 are also important for clubroot development, as *P. brassicae* produces small amounts of cytokinins itself
369 and impairs the host cytokinin degradation pathway [8], [33]. Even though the majority of host genes
370 involved in the synthesis of cytokinins are downregulated in wild-type *A. thaliana* during clubroot disease
371 at 16 DAI [31] (confirmed by our experiment), endogenous production and decreased degradation argue
372 in favour of *P. brassicae*'s need for cytokinins at the local level. Recent findings show that *P. brassicae*
373 GRETCHEN HAGEN 3 (PbGH3) protein may be involved in the conversion and inactivation of host auxins
374 [23], which can act as suppressors of amyloplast differentiation [84].

375 Albeit speculative, it is possible that the increased PPR protein-driven RNA modification in infected root
376 tissue may be connected to *P. brassicae* infection leading to the transformation of root proplastids into
377 amyloplasts, enabling the storage of sugars directed toward the infection-induced sink tissue [6], [85]. This
378 hypothesis is further supported by the fact that *Arabidopsis* stores starch in its leaves during the day and
379 mobilizes it during the night to supply sink tissues, including the rapidly growing root [38], [40], [41]. In our
380 hypothetical scenario the parasite alters the cytokinins-to-auxins ratio redirecting sugars meant for root
381 growth during the night to amyloplasts, where they are stored as constant energy supply for the growing
382 pathogen. This hypothesis is supported by observable phenotypical changes in infected tissue (i.e.,
383 amyloplast formation and accumulation in infected cells), but many DEGs in the category "RNA
384 modification" are also involved in putative editing of mitochondrial RNA. The most upregulated gene
385 within the category encodes a mitochondrial RNA editing PPR, LOVASTATINE INSENSITIVE 1 (LOI1), which

386 appears to play a role in the regulation of isoprenoid biosynthesis [86], a category also enriched in our
387 analysis of the night phase of intermediate infection ("Isoprenoid biosynthetic process", Fig. 2 B). RNA
388 editing in mitochondria and chloroplasts can impact numerous downstream processes beyond the
389 targeted organelles. This is exemplified by a recent report of an organellar RNA-editing factor negatively
390 affecting resistance of *Nicotiana benthamiana* to *Phythophthora* spp. [87], highlighting the need for
391 experimental studies to dissect, validate and understand the role of clubroot induced RNA editing during
392 the night in order to verify or falsify the above developed hypothesis.

393 The IE model allowed for the detection of a small and interesting subset of DEGs whose expression pattern
394 is simultaneously affected by time of the day and infection [64]. The overall reduction of DEGs at 21 DAI
395 as compared to 14 DAI (i.e., 96 against 217) is likely due to the already observed decreased effect of diel
396 oscillations in older plants and explains the absence of day/night grouping of the samples at 21 DAI (Fig.
397 5). At 14 DAI, when the effect of time on gene expression is stronger, DEGs appropriately divide samples
398 into day/night and infected/control groups (Fig. 4). At 14 DAI, row clustering reveals varying effects of
399 infection on the diel gene expression patterns, the most notable being the suppression of rhythmicity
400 through upregulation of genes that are normally downregulated at night (i.e., cluster 1 in Fig. 4).
401 Interestingly, the GO term enrichment analysis of the DEGs in cluster 1 features the terms "Circadian
402 rhythm" and "Rhythmic process" (Additional File 5). A closer look at the list of genes contained in cluster
403 1 revealed seven genes of acknowledged importance in rhythmic and circadian processes: *GIGANTEA* (GI),
404 *PSEUDO-RESPONSE REGULATOR* 3 (PRR3), 7 (PRR7) and 9 (PRR9); *PHYTOCHROME INTERACTING FACTOR*
405 *4* (PIF4), *NIGHT LIGHT-INDUCIBLE AND CLOCK-REGULATED* 1 (LNK1) and 4 (LNK4). Members of the core
406 circadian clock such as GI and the PRRs are known to be directly involved in the
407 transcriptional/translational feedback loop central to circadian oscillations [36], but also to integrate
408 endogenous and exogenous stimuli to inform and entrain it [37], a role they share with PIF4 and LNK1/4
409 [88], [89]. Whilst LNK1 and LNK4 seems to mainly integrate temperature stimuli in the circadian oscillator

410 [89], all other genes detected above are variously involved in the integration of information about
411 temperature, light, sugar and hormone levels within the circadian clock [37]. While temperature and light
412 are unlikely to be involved in mediating the pathogen influence on the diel rhythm of the host, *P. brassicae*
413 influence on hormones [90], [91] and sugar levels [80], [85] is documented and a more plausible mediator.
414 Considering the suppression of the diel cycle observed in cluster 1 and the fact that the majority of the
415 rhythmic genes we identified within it are inhibitors of the central oscillator CIRCADIAN CLOCK
416 ASSOCIATED 1 / LATE ELONGATED HYPOCOTYL (CCA1/LHY), either directly such as PRR9, PRR7 [92] or
417 indirectly such as PRR3 (via TOC1; [93]) and LNK1 (via RVE8 and PRR5; [89]), it is possible that these genes
418 are mediating the influence of the pathogen on the circadian clock.

419 In the shoot PRR7 is activated in condition of low sugars by a mechanism involving the activation of the
420 sugar sensor SUCROSE NON FERMENTING RELATED KINASE 1 (SnRK1), itself phosphorylating the
421 transcription factor bZIP63 which activates PRR7 transcription [94]. Interestingly, SnRK1 has been found
422 to be the direct target of the recently described *P. brassicae*-specific effector protein PBZF1 [95]. SnRK1 is
423 a central sensor of nutrient stress in plants [96], and the fact that this gene seems to be at the center of
424 direct (i.e., via effectors) and indirect (i.e., via changes in sugar levels) manipulation by *P. brassicae* argues
425 for its pivotal role in the interaction. Recent studies have shown that sucrose has an even higher
426 importance in conveying circadian information in the root, where sucrose pulses from the shoot regulate
427 diel oscillations of PRR7 (and PRR9) [97]. Building on our previous hypothesis, we speculate that the
428 parasite influences the rhythmic processes of its host indirectly, by promoting the sequestration of the
429 sugars in amyloplastic starch for later consumption. Unlike sucrose and trehalose-6-phosphate levels,
430 plants do not regulate starch turnover based on its abundance [98]. As a result, the parasites direct
431 consumption of sucrose or the induction of amyloplastic storage could create a continuous flow of
432 photosynthates towards the infection-induced sink, disrupting the normal rhythmic pattern of sugar
433 delivery to the root. This scenario of a nutrient deprived tissue with consistent expression of PRR7 is

434 further supported in our study by the high expression of the “starvation gene” SKIP20 (a.k.a. KMD4 or
435 At3g59940; [38]) in infected roots.

436 Despite showing expression patterns like the one discussed above, GI and PIF4 are less clearly influenced
437 by sugar metabolism. Sucrose pulses in sugar-depleted condition in the dark are known to be able to re-
438 establish the oscillations of the circadian clock by post-transcriptionally stabilizing GI but they do not
439 change its expression levels [99], [100]; whilst sucrose influences the expression pattern of various PIFs,
440 but not of PIF4 [101]. GI is a plant specific circadian protein promoting the transcription of thousands of
441 genes and whose competitive interaction with PIF4 integrates endogenous oscillations with light and
442 temperature in order to optimize growth [102], [103]. Among the many processes influenced by GI,
443 senescence is particularly interesting, since it is also found in our GO term enrichment analysis of cluster
444 1 (“Plant organ senescence”; “Leaf senescence”; Additional File 5) and prior studies have shown delayed
445 senescence when *GI* expression is suppressed [104].

446 In our dataset, the established connection between circadian rhythms and senescence processes may be
447 linked to the continuous expression of *GI* during the night, explaining the premature senescence and the
448 yellowing of leaves observed as typical clubroot symptoms. GI nocturnal breakdown also regulates
449 gibberellin mediated growth by allowing DELLA degradation and enabling the expression of downstream
450 growth promoting genes [105]. The upregulation of *GI* in the night in our dataset might therefore be
451 involved in disrupting the root growth (especially lateral root formation and main root elongation) by
452 making cells insensitive to gibberellin [106]. Intriguingly, GI is also involved in stabilization of REPRESSOR
453 OF GA (RGA; [103]), itself inhibiting the gibberellin-induced transcription of PIF4 (another promoter of
454 growth genes), which is instead upregulated in the night in infected plants. These results highlight the
455 complexity of the influence of the circadian oscillator on downstream processes acting at the post-
456 transcriptional level.

These findings suggest that *P. brassicae* disrupts host circadian processes through direct and indirect mechanisms, including sugar consumption and hormone manipulation. Direct manipulation by the parasite is likely to have adapted to the diel oscillations of the host and ongoing analyses of the diel changes in gene expression on the side of the parasite might help highlight time-specific effectors. Furthermore, our investigation already revealed how circadian oscillations in gene expression (i.e., oscillations at a finer scale than the day and night) are also altered by *P. brassicae* and tools for the analysis of differential rhythmicity will be applied to further explore the influence of clubroot on plant circadian processes. A more in-depth exploration of this complex dataset will have to continue in a targeted "gene-by-gene" way, in order to provide questions amenable for experimental validation on the time-specific cross-talk between *P. brassicae* and its host. Furthermore, the occurrence in our analysis of terms such as "Circadian rhythm" already points toward the next step of our investigation, where the influence of clubroot infection on the rhythmic oscillations of circadian genes will be dissected.

Acknowledgements

We are grateful to Bettina Schneidhofer for her support in the wet lab. We would also like to thank the VBCF NGS Unit (www.vbcf.ac.at) in particular Carmen Czepe for her support during the sequencing and Nadine Tatto for her paramount contribution and continuous support with the bioinformatic analyses.

Authors' contribution

Experimental concept and design: SN, JLM. Wet lab work: SA, FB, AG, MH. Bioinformatics and statistical analysis: AG. Analysis of Results: AG, SN, SA, JLM, MH. Manuscript writing: AG, SN, SA, JLM. Figures and tables: AG. All authors read and approved the final manuscript.

Funding

This research was funded in whole by the Austrian Science Fund (FWF) [grant DOI:10.55776/Y801]. For open access purposes, the authors have applied a CC BY public copyright license to any author accepted manuscript version arising from this submission.

Availability of data and materials

Raw NGS sequences of the dataset generated and analysed in the current study are available in NCBI Sequence Read Archive (SRA) under the BioProject accession number PRJNA1212907 or are available from the corresponding author on request.

Ethics approval and consent to participate

Not applicable.

Consent for publication

Not applicable.

Competing interests

The authors declare that they have no competing interests.

Author details

[1]Institut für Mikrobiologie, Universität Innsbruck, Technikerstraße 25, 6020 Innsbruck, Tirol, Austria. [2]Faculty of Biology, Technische Universität Dresden, 01062 Dresden, Germany.

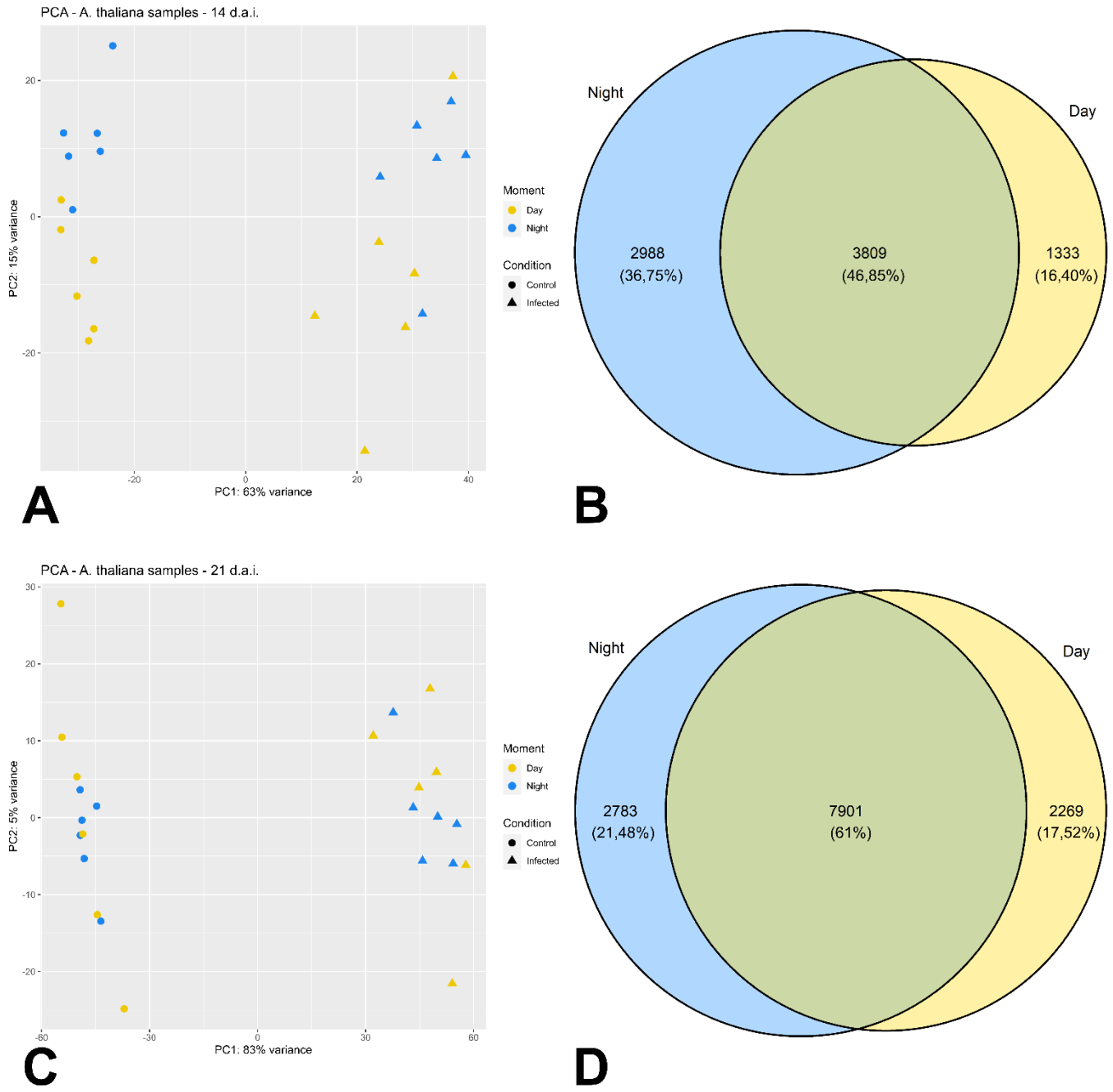

Fig. 1 Day/night-informed overview of gene expression in samples of A. thaliana roots 14 DAI (A, B) and 21 DAI (C, D) with P. brassicae. A and C, PCA of A. thaliana root samples structured by gene expression estimates (i.e., vst counts). B and D, Proportions of DE genes between infected and healthy A. thaliana roots assigned to the day, night or both.

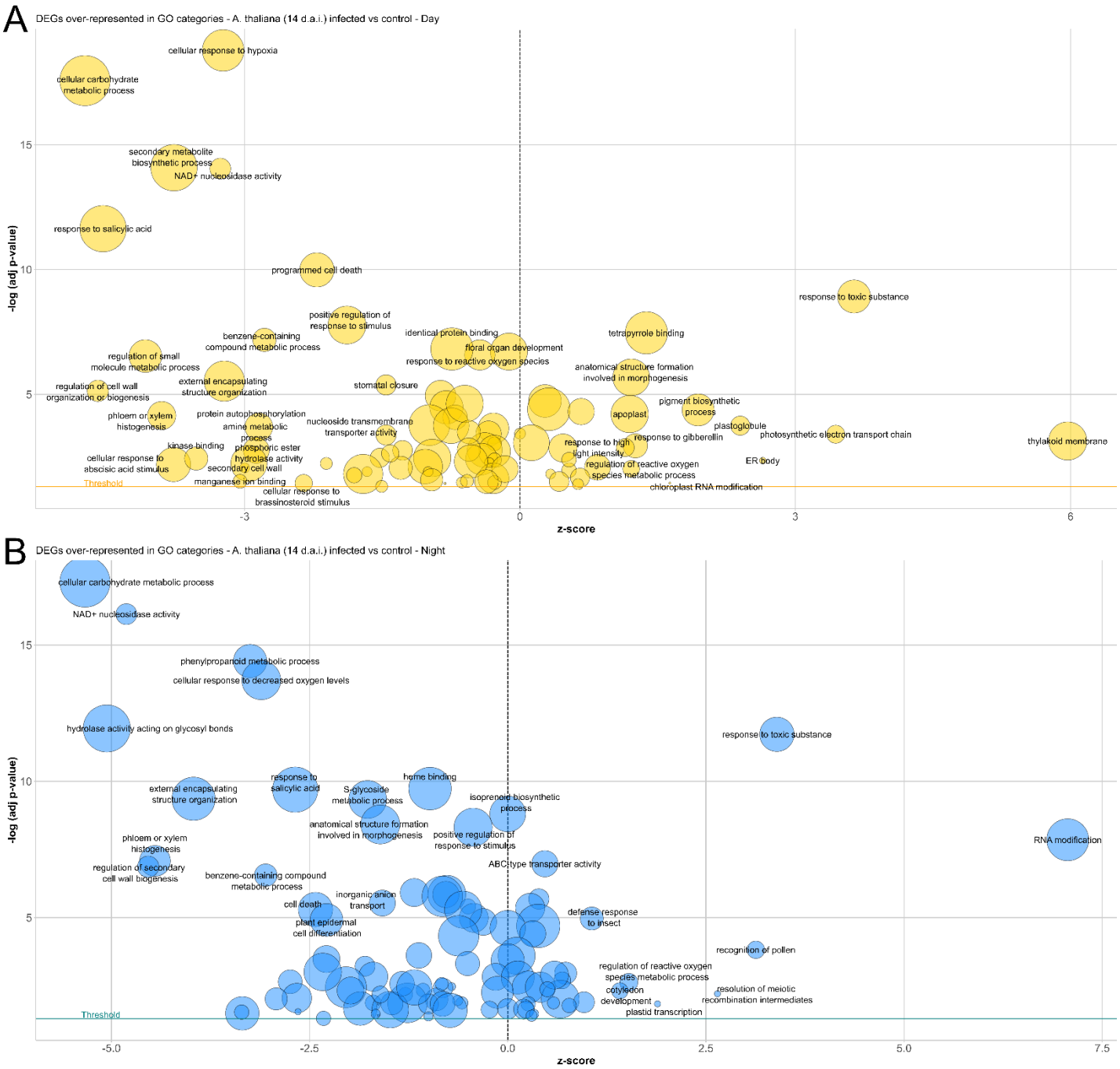

Fig. 2 GO bubble chart of GO categories enriched in DEGs in infected A. thaliana roots during the day (A, yellow) and night (B, blue) 14 DAI by P. brassicae. The bubbles are arranged according to their overall expression level or z-score on the x axis and according to the negative logarithmic scale of the adjusted p-value on the y axis. The bubble size is proportional to the gene counts within each category. The significance threshold of adjusted p-value < 0,05 (1,3 in -log10 scale) is represented by coloured lines parallel to the x axis (orange in the day and turquoise in the night).

512

513 *Table 1: All GO categories enriched in DEGs in A. thaliana roots 14 DAI infected by P. brassicae as in Fig 3. GO categories are*
514 *organised by decreasing -log10 adjusted p-value (i.e., top to bottom in the relative figure).*

GO term categories affected by *P.brassicae* infection in *A. thaliana* 14 d.a.i.									
Day					**Night**				
Upregulated									
ID	**term**	**count**	**adj_pval**	**zscore**	**ID**	**term**	**count**	**adj_pval**	**zscore**
GO:0009636	response to toxic substance	55	8,92	3,64	GO:0009636	response to toxic substance	68	11,73	3,40
GO:0046906	tetrapyrrole binding	89	7,47	1,38	GO:0009451	RNA modification	101	7,86	7,06
GO:0048646	anatomical structure formation involved in morphogenesis	68	5,68	1,21	GO:0140359	ABC-type transporter activity	41	6,98	0,47
GO:0008299	isoprenoid biosynthetic process	54	4,74	0,27	GO:0090332	stomatal closure	26	5,69	0,39
GO:0048580	regulation of post-embryonic development	91	4,41	0,31	GO:0000302	response to reactive oxygen species	50	5,36	0,28
GO:0046148	pigment biosynthetic process	52	4,38	1,94	GO:0002213	defense response to insect	32	4,97	1,06
GO:0038023	signaling receptor activity	36	4,31	0,67	GO:0048580	regulation of post-embryonic development	108	4,70	0,38
GO:0048046	apoplast	70	4,22	1,20	GO:0009739	response to gibberellin	40	4,41	0,32
GO:0010287	plastoglobule	21	3,75	2,40	GO:0048544	recognition of pollen	20	3,82	3,13
GO:0009767	photosynthetic electron transport chain	19	3,41	3,44	GO:0009991	response to extracellular stimulus	79	3,60	0,11
GO:0042651	thylakoid membrane	73	3,14	5,97	GO:0045165	cell fate commitment	30	2,96	0,73
GO:0016829	lyase activity	65	3,06	0,12	GO:0099503	secretory vesicle	46	2,90	0,59
GO:0009739	response to gibberellin	31	2,94	1,26	GO:0071214	cellular response to abiotic stimulus	63	2,81	0,13
GO:0009644	response to high light intensity	19	2,87	1,15	GO:0007166	cell surface receptor signaling pathway	19	2,70	0,69
GO:0015267	channel activity	41	2,86	0,47	GO:2000377	regulation of reactive oxygen species metabolic process	21	2,63	1,53
GO:0102483	scopolin beta-glucosidase activity	14	2,39	0,53	GO:0009723	response to ethylene	60	2,45	0,26
GO:0010168	ER body	7	2,35	2,65	GO:1902679	negative regulation of RNA biosynthetic process	53	2,45	0,41
GO:0016054	organic acid catabolic process	35	2,09	0,85	GO:0008171	O-methyltransferase activity	16	2,38	0,50
GO:2000377	regulation of reactive oxygen species metabolic process	17	2,02	1,21	GO:0048825	cotyledon development	18	2,32	1,41
GO:0048544	recognition of pollen	14	1,96	0,53	GO:0000712	resolution of meiotic recombination intermediates	7	2,21	2,65
GO:0000373	Group II intron splicing	9	1,82	0,33	GO:0042440	pigment metabolic process	82	2,01	0,66
GO:0009630	gravitropism	21	1,66	0,65	GO:0008283	cell population proliferation	27	1,90	0,96
GO:0008283	cell population proliferation	22	1,51	0,43	GO:0048235	pollen sperm cell differentiation	12	1,87	0,58
GO:1900865	chloroplast RNA modification	6	1,45	1,63	GO:0000079	regulation of cyclin-dependent protein	15	1,84	0,26

						serine/threonine kinase activity			
GO:0006638	neutral lipid metabolic process	10	1,41	0,63	GO:0042793	plastid transcription	7	1,84	1,89
					GO:0002832	negative regulation of response to biotic stimulus	15	1,78	0,77
					GO:0010114	response to red light	25	1,64	0,20
					GO:0010090	trichome morphogenesis	19	1,63	0,23
					GO:0019432	triglyceride biosynthetic process	9	1,47	0,33
					GO:1901681	sulfur compound binding	11	1,40	0,30
Zero z-score									
ID	**term**	**count**	**adj_pval**	**zscore**	**ID**	**term**	**count**	**adj_pval**	**zscore**
GO:0002238	response to molecule of fungal origin	10	3,43	0,00	GO:0008299	isoprenoid biosynthetic process	74	8,81	0,00
					GO:0048437	floral organ development	72	4,62	0,00
					GO:1901698	response to nitrogen compound	64	3,43	0,00
					GO:0009608	response to symbiont	6	1,75	0,00
					GO:0009629	response to gravity	26	1,66	0,00
Downregulated									
ID	**term**	**count**	**adj_pval**	**zscore**	**ID**	**term**	**count**	**adj_pval**	**zscore**
GO:0071456	cellular response to hypoxia	86	18,78	-3,23	GO:0044262	cellular carbohydrate metabolic process	144	17,31	-5,33
GO:0044262	cellular carbohydrate metabolic process	125	17,57	-4,74	GO:0003953	NAD+ nucleosidase activity	27	16,14	-4,81
GO:0044550	secondary metabolite biosynthetic process	107	14,08	-3,77	GO:0009698	phenylpropanoid metabolic process	64	14,42	-3,25
GO:0003953	NAD+ nucleosidase activity	24	14,04	-3,27	GO:0036294	cellular response to decreased oxygen levels	87	13,71	-3,11
GO:0009751	response to salicylic acid	107	11,64	-4,54	GO:0016798	hydrolase activity acting on glycosyl bonds	127	11,94	-5,06
GO:0012501	programmed cell death	59	9,99	-2,21	GO:0020037	heme binding	104	9,74	-0,98
GO:0048584	positive regulation of response to stimulus	72	7,78	-1,89	GO:0009751	response to salicylic acid	117	9,70	-2,68
GO:0042537	benzene-containing compound metabolic process	29	7,18	-2,79	GO:0045229	external encapsulating structure organization	107	9,36	-3,96
GO:0042802	identical protein binding	89	6,82	-0,74	GO:0016143	S-glycoside metabolic process	82	9,34	-1,77
GO:0048437	floral organ development	69	6,71	-0,12	GO:0048646	anatomical structure formation involved in morphogenesis	87	8,42	-1,61
GO:0000302	response to reactive oxygen species	47	6,58	-0,44	GO:0048584	positive regulation of response to stimulus	84	8,32	-0,44
GO:0062012	regulation of small molecule metabolic process	54	6,54	-4,08	GO:0010087	phloem or xylem histogenesis	55	7,08	-4,45
GO:0045229	external encapsulating structure organization	81	5,53	-3,22	GO:2000652	regulation of secondary cell wall biogenesis	28	6,87	-4,54
GO:0090332	stomatal closure	23	5,38	-1,46	GO:0042537	benzene-containing compound metabolic process	31	6,56	-3,05

GO:1903338	regulation of cell wall organization or biogenesis	25	5,14	-4,60	GO:0015849	organic acid transport	46	5,92	-1,18
GO:0009743	response to carbohydrate	48	4,95	-0,87	GO:0010150	leaf senescence	83	5,86	-0,77
GO:0016747	acyltransferase activity transferring groups other than amino-acyl groups	69	4,63	-0,60	GO:0010648	negative regulation of cell communication	41	5,85	-0,78
GO:0048585	negative regulation of response to stimulus	56	4,49	-0,80	GO:0006811	monoatomic ion transport	94	5,78	-0,83
GO:0010087	phloem or xylem histogenesis	41	4,16	-3,90	GO:0015698	inorganic anion transport	40	5,54	-1,58
GO:0015698	inorganic anion transport	32	4,09	-0,71	GO:0010143	cutin biosynthetic process	16	5,41	-0,50
GO:0009733	response to auxin	83	3,77	-0,99	GO:0008219	cell death	68	5,30	-2,43
GO:0010150	leaf senescence	64	3,75	-0,75	GO:0000981	DNA-binding transcription factor activity RNA polymerase II-specific	79	5,30	-0,56
GO:0046777	protein autophosphorylation	40	3,70	-2,85	GO:0007623	circadian rhythm	49	4,99	-0,43
GO:0042594	response to starvation	48	3,64	-0,29	GO:0090627	plant epidermal cell differentiation	62	4,92	-2,29
GO:0140359	ABC-type transporter activity	29	3,49	-0,56	GO:0071365	cellular response to auxin stimulus	42	4,84	-0,31
GO:0015849	organic acid transport	34	3,43	-0,34	GO:0042802	identical protein binding	94	4,33	-0,62
GO:0006816	calcium ion transport	23	3,38	-1,46	GO:0009735	response to cytokinin	39	3,62	-1,12
GO:0048235	pollen sperm cell differentiation	13	3,02	-0,28	GO:0009308	amine metabolic process	43	3,48	-2,29
GO:0070417	cellular response to cold	13	3,02	-0,28	GO:0043621	protein self-association	35	3,32	-0,51
GO:0043621	protein self-association	29	2,79	-0,56	GO:0034285	response to disaccharide	25	3,22	-1,80
GO:0006631	fatty acid metabolic process	61	2,77	-0,38	GO:0019899	enzyme binding	81	3,01	-2,33
GO:0009308	amine metabolic process	35	2,76	-2,87	GO:0022603	regulation of anatomical structure morphogenesis	50	2,84	-1,70
GO:0009624	response to nematode	22	2,76	-1,28	GO:0046777	protein autophosphorylation	43	2,83	-0,15
GO:1901698	response to nitrogen compound	52	2,72	-0,28	GO:0009741	response to brassinosteroid	34	2,65	-2,74
GO:0042887	amide transmembrane transporter activity	18	2,64	-1,41	GO:0009705	plant-type vacuole membrane	36	2,58	-1,33
GO:0048767	root hair elongation	21	2,46	-1,53	GO:0015295	solute:proton symporter activity	13	2,57	-0,83
GO:0009408	response to heat	70	2,46	-0,96	GO:0006880	intracellular sequestering of iron ion	8	2,47	-0,71
GO:0019900	kinase binding	29	2,43	-3,53	GO:0009826	unidimensional cell growth	96	2,45	-2,04
GO:0010073	meristem maintenance	51	2,41	-0,42	GO:0048046	apoplast	72	2,44	-1,18
GO:0009625	response to insect	13	2,38	-0,28	GO:0009624	response to nematode	24	2,42	-0,82
GO:0000981	DNA-binding transcription factor activity RNA polymerase II-specific	56	2,32	-0,53	GO:0006833	water transport	14	2,34	-1,07
GO:0051644	plastid localization	9	2,27	-0,33	GO:0008236	serine-type peptidase activity	43	2,33	-1,98

GO:0005337	nucleoside transmembrane transporter activity	11	2,24	-2,11	GO:0010073	meristem maintenance	59	2,26	-0,13
GO:0042578	phosphoric ester hydrolase activity	66	2,24	-2,95	GO:0051119	sugar transmembrane transporter activity	19	2,18	-1,61
GO:0071215	cellular response to abscisic acid stimulus	59	2,19	-3,78	GO:0042886	amide transport	15	2,18	-1,29
GO:0007389	pattern specification process	60	2,11	-1,03	GO:0010038	response to metal ion	51	2,05	-2,66
GO:0009705	plant-type vacuole membrane	29	2,06	-1,30	GO:0008374	O-acyltransferase activity	30	2,02	-2,92
GO:0009531	secondary cell wall	9	2,06	-3,00	GO:0009411	response to UV	31	2,00	-0,90
GO:0005507	copper ion binding	37	2,01	-0,16	GO:0030570	pectate lyase activity	10	1,96	-0,63
GO:0055062	phosphate ion homeostasis	9	1,91	-1,00	GO:0070417	cellular response to cold	12	1,87	-0,58
GO:0009269	response to desiccation	9	1,91	-1,67	GO:0035556	intracellular signal transduction	90	1,87	-1,26
GO:0009826	unidimensional cell growth	77	1,82	-1,71	GO:0010214	seed coat development	17	1,87	-1,70
GO:0004620	phospholipase activity	15	1,76	-1,81	GO:0051049	regulation of transport	30	1,85	-1,46
GO:0071214	cellular response to abiotic stimulus	48	1,64	-0,29	GO:0050660	flavin adenine dinucleotide binding	37	1,84	-0,82
GO:0009735	response to cytokinin	27	1,58	-0,96	GO:0004551	dinucleotide phosphatase activity	6	1,84	-1,63
GO:0008171	O-methyltransferase activity	12	1,53	-0,58	GO:0009615	response to virus	25	1,83	-1,00
GO:0030145	manganese ion binding	13	1,52	-3,05	GO:0006631	fatty acid metabolic process	65	1,67	-1,86
GO:0050660	flavin adenine dinucleotide binding	30	1,51	-0,37	GO:0009850	auxin metabolic process	19	1,63	-0,23
GO:0040034	regulation of development heterochronic	13	1,47	-0,28	GO:0009408	response to heat	77	1,63	-1,48
GO:0045926	negative regulation of growth	10	1,47	-0,63	GO:0016829	lyase activity	68	1,60	-0,73
GO:0071367	cellular response to brassinosteroid stimulus	18	1,45	-2,36	GO:0051923	sulfation	7	1,55	-2,65
GO:0016307	phosphatidylinositol phosphate kinase activity	6	1,43	-0,82	GO:0030145	manganese ion binding	15	1,54	-3,36
GO:0015081	sodium ion transmembrane transporter activity	11	1,32	-1,51	GO:0007010	cytoskeleton organization	65	1,49	-3,35
					GO:0009269	response to desiccation	9	1,47	-1,67
					GO:0090158	endoplasmic reticulum membrane organization	6	1,42	-1,63
					GO:0015851	nucleobase transport	9	1,38	-1,00
					GO:0009631	cold acclimation	15	1,31	-2,32

515

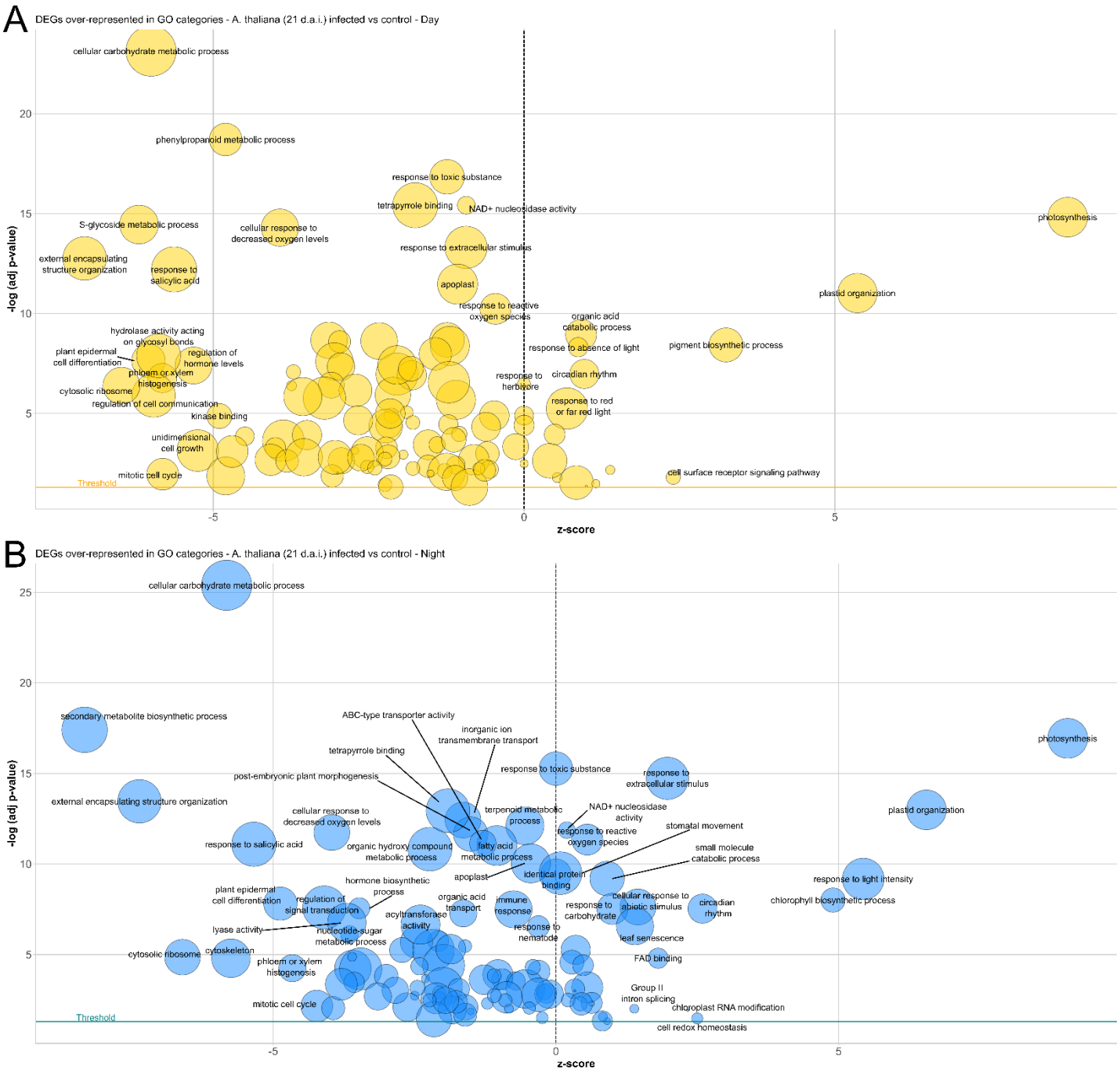

Fig. 3 GO bubble chart of GO categories enriched in DEGs in infected A. thaliana roots during the day (top, yellow) and night (blue, bottom) 21 DAI by P. brassicae. The bubbles are arranged according to their overall expression level or z-score on the x axis and according to the negative logarithmic scale of the adjusted p-value on the y axis. The bubble size is proportional to the gene counts within each category. The significance threshold of adjusted p-value < 0,05 (1,3 in -log10 scale) is represented by coloured lines parallel to the x axis (orange in the day and turquoise in the night).

526 *Table 2: All GO categories enriched in DEGs in infected A. thaliana roots 21 DAI by P. brassicae as in Fig 3. GO categories are*
527 *organised by decreasing -log10 adjusted p-value (i.e., top to bottom in the relative figure).*

GO term categories affected by *P.brassicae* infection in *A. thaliana* 21 d.a.i.									
Day					**Night**				
Upregulated									
ID	**term**	**count**	**adj_pval**	**zscore**	**ID**	**term**	**count**	**adj_pval**	**zscore**
GO:0015979	photosynthesis	123	14,82	8,75	GO:0015979	photosynthesis	132	16,94	9,05
GO:0009657	plastid organization	121	11,02	5,36	GO:0009991	response to extracellular stimulus	148	14,73	1,97
GO:0016054	organic acid catabolic process	76	8,94	0,92	GO:0009657	plastid organization	131	12,99	6,55
GO:0046148	pigment biosynthetic process	91	8,43	3,25	GO:0003953	NAD+ nucleosidase activity	27	11,87	0,19
GO:0009646	response to absence of light	33	8,32	0,87	GO:0000302	response to reactive oxygen species	81	11,34	0,56
GO:0007623	circadian rhythm	68	6,98	0,97	GO:0042802	identical protein binding	151	9,49	0,08
GO:0009639	response to red or far red light	134	5,25	0,69	GO:0044282	small molecule catabolic process	99	9,20	0,90
GO:0002213	defense response to insect	37	3,95	0,49	GO:0009642	response to light intensity	143	9,17	5,44
GO:0005777	peroxisome	94	2,63	0,41	GO:0015995	chlorophyll biosynthetic process	51	8,01	4,90
GO:0000373	Group II intron splicing	13	2,17	1,39	GO:0071214	cellular response to abiotic stimulus	107	7,63	1,45
GO:0007166	cell surface receptor signaling pathway	21	1,81	2,40	GO:0007623	circadian rhythm	72	7,53	2,59
GO:0006641	triglyceride metabolic process	14	1,79	0,53	GO:0009743	response to carbohydrate	81	7,52	1,00
GO:1901361	organic cyclic compound catabolic process	90	1,55	0,84	GO:0010150	leaf senescence	115	6,56	1,40
GO:0015749	monosaccharide transmembrane transport	12	1,49	1,15	GO:0051093	negative regulation of developmental process	73	5,26	0,35
GO:0005315	inorganic phosphate transmembrane transporter activity	9	1,35	1,00	GO:0071949	FAD binding	37	4,80	1,81
					GO:0043621	protein self-association	50	4,58	0,28
					GO:0015144	carbohydrate transmembrane transporter activity	39	4,41	0,48
					GO:0051253	negative regulation of RNA metabolic process	81	3,19	0,56

					GO:0 0022 13	defense response to insect	36	3,10	0,33
					GO:0 0082 71	secondary active sulfate transmembrane transporter activity	9	3,00	0,33
					GO:0 0100 14	meristem initiation	21	2,49	0,22
					GO:0 0224 11	cellular component disassembly	40	2,33	0,63
					GO:0 0097 04	de-etiolation	10	2,29	0,63
					GO:0 0400 34	regulation of development heterochronic	22	2,28	0,43
					GO:0 0097 39	response to gibberellin	45	2,28	0,45
					GO:0 0003 73	Group II intron splicing	13	2,01	1,39
					GO:1 9008 65	chloroplast RNA modification	9	1,92	2,33
					GO:0 0101 81	FMN binding	13	1,57	0,83
					GO:0 0454 54	cell redox homeostasis	16	1,48	2,50
					GO:0 0314 06	carboxylic acid binding	37	1,33	0,82
					GO:0 0194 32	triglyceride biosynthetic process	11	1,32	0,90
Zero z-score									
ID	**term**	**count**	**adj_pval**	**zscore**	**ID**	**term**	**count**	**adj_pval**	**zscore**
GO:00 80027	response to herbivore	18	6,49	0	GO:0 0096 36	response to toxic substance	94	15,27	0
GO:19 01699	cellular response to nitrogen compound	32	4,90	0	GO:0 0101 18	stomatal movement	78	9,44	0
GO:00 09624	response to nematode	36	4,40	0					
GO:00 04033	aldo-keto reductase (NADP) activity	12	2,49	0					
Downregulated									
ID	**term**	**count**	**adj_pval**	**zscore**	**ID**	**term**	**count**	**adj_pval**	**zscore**
GO:00 44262	cellular carbohydrate metabolic process	196	23,13	-6,00	GO:0 0442 62	cellular carbohydrate metabolic process	208	25,39	-5,82
GO:00 09698	phenylpropanoid metabolic process	84	18,71	-4,80	GO:0 0445 50	secondary metabolite biosynthetic process	171	17,41	-8,34

GO:0009636	response to toxic substance	94	16,84	-1,24	GO:0045229	external encapsulating structure organization	156	13,46	-7,37
GO:0003953	NAD+ nucleosidase activity	29	15,42	-0,93	GO:0046906	tetrapyrrole binding	158	12,94	-1,91
GO:0046906	tetrapyrrole binding	158	15,42	-1,75	GO:0098660	inorganic ion transmembrane transport	107	12,43	-1,64
GO:0016143	S-glycoside metabolic process	117	14,45	-6,19	GO:0006721	terpenoid metabolic process	120	12,11	-0,55
GO:0036294	cellular response to decreased oxygen levels	109	14,30	-3,93	GO:0036294	cellular response to decreased oxygen levels	107	11,74	-3,96
GO:0009991	response to extracellular stimulus	139	13,31	-0,93	GO:0090698	post-embryonic plant morphogenesis	99	11,65	-1,51
GO:0045229	external encapsulating structure organization	148	12,76	-7,07	GO:0140359	ABC-type transporter activity	60	11,13	-1,29
GO:0009751	response to salicylic acid	159	12,21	-5,63	GO:0009751	response to salicylic acid	162	11,09	-5,34
GO:0048046	apoplast	126	11,47	-1,07	GO:0006631	fatty acid metabolic process	132	11,01	-1,04
GO:0000302	response to reactive oxygen species	76	10,23	-0,46	GO:1901615	organic hydroxy compound metabolic process	158	10,82	-2,23
GO:0098660	inorganic ion transmembrane transport	94	8,68	-1,24	GO:0048046	apoplast	127	10,03	-0,44
GO:0010016	shoot system morphogenesis	104	8,66	-3,14	GO:0090627	plant epidermal cell differentiation	93	7,81	-4,87
GO:0006721	terpenoid metabolic process	106	8,62	-2,33	GO:0009966	regulation of signal transduction	155	7,60	-4,10
GO:0042537	benzene-containing compound metabolic process	41	8,59	-2,97	GO:0042446	hormone biosynthetic process	40	7,56	-3,48
GO:0006631	fatty acid metabolic process	119	8,38	-1,19	GO:0006955	immune response	114	7,50	-0,75
GO:0090696	post-embryonic plant organ development	83	7,98	-1,43	GO:0015849	organic acid transport	63	7,27	-1,64
GO:0016798	hydrolase activity acting on glycosyl bonds	150	7,89	-5,88	GO:0016829	lyase activity	123	6,77	-3,70
GO:0090627	plant epidermal cell differentiation	89	7,64	-6,04	GO:0016746	acyltransferase activity	127	6,66	-2,40
GO:0006955	immune response	110	7,60	-3,05	GO:0009624	response to nematode	42	6,55	-0,31
GO:0016747	acyltransferase activity transferring groups other than amino-acyl groups	116	7,43	-2,04	GO:0009225	nucleotide-sugar metabolic process	30	6,10	-3,65
GO:0010817	regulation of hormone levels	107	7,40	-5,32	GO:2000280	regulation of root development	39	5,74	-2,08

GO:0015849	organic acid transport	61	7,34	-2,94	GO:0010038	response to metal ion	87	5,69	-2,47
GO:0140359	ABC-type transporter activity	51	7,24	-1,82	GO:0010143	cutin biosynthetic process	19	5,47	-1,61
GO:0016682	oxidoreductase activity acting on diphenols and related substances as donors oxygen as acceptor	21	7,08	-3,71	GO:0015267	channel activity	74	5,30	-1,86
GO:1901615	organic hydroxy compound metabolic process	138	6,97	-2,04	GO:0009741	response to brassinosteroid	54	5,25	-2,72
GO:0010118	stomatal movement	69	6,91	-1,81	GO:0009733	response to auxin	144	5,24	-2,17
GO:0010087	phloem or xylem histogenesis	68	6,77	-5,82	GO:0048226	Casparian strip	13	4,87	-3,61
GO:0042802	identical protein binding	134	6,56	-1,21	GO:0022626	cytosolic ribosome	106	4,85	-6,60
GO:0009741	response to brassinosteroid	55	6,42	-3,10	GO:0005856	cytoskeleton	124	4,80	-5,75
GO:0048226	Casparian strip	14	6,39	-3,74	GO:0035556	intracellular signal transduction	146	4,40	-1,99
GO:0022626	cytosolic ribosome	107	6,39	-6,48	GO:0004620	phospholipase activity	29	4,35	-2,41
GO:0010038	response to metal ion	85	6,15	-2,71	GO:0102483	scopolin beta-glucosidase activity	24	4,31	-0,41
GO:0048437	floral organ development	99	5,92	-2,11	GO:0010087	phloem or xylem histogenesis	63	4,25	-4,66
GO:0010646	regulation of cell communication	146	5,90	-5,96	GO:0007389	pattern specification process	112	4,23	-3,59
GO:0016829	lyase activity	114	5,84	-3,56	GO:0009826	unidimensional cell growth	148	4,20	-3,45
GO:0009733	response to auxin	140	5,77	-3,21	GO:0008283	cell population proliferation	44	4,07	-0,30
GO:0090693	plant organ senescence	120	5,68	-1,10	GO:0048438	floral whorl development	77	3,89	-1,03
GO:0010143	cutin biosynthetic process	18	5,06	-1,89	GO:1904680	peptide transmembrane transporter activity	21	3,83	-1,09
GO:0015267	channel activity	70	5,00	-2,15	GO:0030029	actin filament-based process	49	3,81	-3,00
GO:0009743	response to carbohydrate	70	4,90	-0,48	GO:0051923	sulfation	12	3,67	-2,31
GO:0006833	water transport	22	4,90	-2,13	GO:0009615	response to virus	40	3,63	-0,95
GO:0019900	kinase binding	51	4,87	-4,90	GO:0090351	seedling development	75	3,61	-1,27

GO:0005507	copper ion binding	68	4,66	-2,67	GO:0006972	hyperosmotic response	32	3,54	-0,71
GO:0070417	cellular response to cold	20	4,55	-1,79	GO:0006576	biogenic amine metabolic process	38	3,47	-3,57
GO:0006972	hyperosmotic response	33	4,45	-1,22	GO:0005509	calcium ion binding	85	3,36	-3,80
GO:0051094	positive regulation of developmental process	54	4,42	-2,18	GO:0009408	response to heat	122	3,23	-1,99
GO:0009723	response to ethylene	89	4,37	-2,23	GO:0030145	manganese ion binding	24	3,16	-2,45
GO:0051093	negative regulation of developmental process	67	4,33	-0,61	GO:0055086	nucleobase-containing small molecule metabolic process	124	3,10	-0,54
GO:0008171	O-methyltransferase activity	23	3,98	-1,04	GO:0009629	response to gravity	41	3,09	-1,72
GO:0005774	vacuolar membrane	69	3,92	-3,49	GO:0099503	secretory vesicle	60	3,03	-2,84
GO:1903338	regulation of cell wall organization or biogenesis	31	3,86	-4,49	GO:0009631	cold acclimation	25	2,94	-0,20
GO:0038023	signaling receptor activity	50	3,68	-1,13	GO:0006833	water transport	19	2,90	-2,06
GO:0035556	intracellular signal transduction	135	3,64	-3,87	GO:0035266	meristem growth	37	2,87	-0,16
GO:1901568	fatty acid derivative metabolic process	25	3,43	-1,40	GO:0016614	oxidoreductase activity acting on CH-OH group of donors	69	2,82	-0,12
GO:0090351	seedling development	71	3,43	-1,54	GO:0000981	DNA-binding transcription factor activity RNA polymerase II-specific	95	2,78	-0,31
GO:0050660	flavin adenine dinucleotide binding	55	3,34	-0,13	GO:0008171	O-methyltransferase activity	21	2,73	-1,09
GO:0008283	cell population proliferation	40	3,29	-2,21	GO:0044273	sulfur compound catabolic process	13	2,73	-2,50
GO:0006576	biogenic amine metabolic process	36	3,28	-4,00	GO:0005507	copper ion binding	63	2,68	-3,15
GO:0009826	unidimensional cell growth	135	3,14	-5,25	GO:1901698	response to nitrogen compound	84	2,64	-0,87
GO:0051923	sulfation	11	3,13	-2,71	GO:0009838	abscission	19	2,59	-2,06
GO:0005509	calcium ion binding	80	3,10	-4,70	GO:0032504	multicellular organism reproduction	81	2,58	-2,11
GO:0010073	meristem maintenance	83	3,03	-2,52	GO:0008236	serine-type peptidase activity	59	2,47	-1,95

GO:0009739	response to gibberellin	46	3,00	-0,59	GO:0042886	amide transport	20	2,47	-0,89
GO:0050829	defense response to Gram-negative bacterium	13	2,94	-1,94	GO:0008378	galactosyltransferase activity	20	2,47	-2,24
GO:0009735	response to cytokinin	47	2,83	-2,19	GO:0005615	extracellular space	46	2,38	-1,77
GO:0000981	DNA-binding transcription factor activity RNA polymerase II-specific	91	2,81	-3,04	GO:0010223	secondary shoot formation	17	2,30	-1,21
GO:0042578	phosphoric ester hydrolase activity	109	2,81	-3,54	GO:0000278	mitotic cell cycle	85	2,16	-4,23
GO:0008236	serine-type peptidase activity	58	2,79	-2,63	GO:0016311	dephosphorylation	70	2,10	-2,63
GO:0008378	galactosyltransferase activity	20	2,72	-2,24	GO:1901607	alpha-amino acid biosynthetic process	56	2,08	-1,60
GO:0051253	negative regulation of RNA metabolic process	75	2,68	-0,81	GO:0019199	transmembrane receptor protein kinase activity	18	2,05	-0,47
GO:0032504	multicellular organism reproduction	78	2,68	-4,08	GO:0044087	regulation of cellular component biogenesis	47	2,04	-3,94
GO:0099503	secretory vesicle	56	2,63	-2,94	GO:0015851	nucleobase transport	13	2,01	-0,83
GO:0030029	actin filament-based process	43	2,62	-3,81	GO:0006644	phospholipid metabolic process	67	1,94	-1,83
GO:0051302	regulation of cell division	30	2,42	-1,10	GO:0003008	system process	11	1,87	-1,51
GO:0009411	response to UV	42	2,36	-1,54	GO:0032879	regulation of localization	47	1,68	-1,60
GO:0042886	amide transport	19	2,33	-2,52	GO:0045927	positive regulation of growth	17	1,51	-0,24
GO:0030145	manganese ion binding	21	2,27	-2,40	GO:0009555	pollen development	104	1,43	-2,16
GO:0000079	regulation of cyclin-dependent protein serine/threonine kinase activity	20	2,25	-1,79					
GO:0015294	solute:monoatomic cation symporter activity	17	2,24	-0,73					
GO:0043094	cellular metabolic compound salvage	29	2,20	-0,56					
GO:0043621	protein self-association	40	2,16	-0,63					
GO:0009631	cold acclimation	22	2,12	-1,28					
GO:0009408	response to heat	109	2,08	-1,25					
GO:0008970	phospholipase A1 activity	9	2,02	-3,00					
GO:0003008	system process	11	2,00	-1,51					
GO:0000278	mitotic cell cycle	80	1,96	-5,81					

GO:00 99080	supramolecular complex	113	1,87	-4,80					
GO:00 05615	extracellular space	42	1,87	-3,09					
GO:19 01607	alpha-amino acid biosynthetic process	52	1,77	-1,11					
GO:00 10214	seed coat development	20	1,44	-2,24					
GO:00 09606	tropism	49	1,32	-2,14					
GO:00 55086	nucleobase-containing small molecule metabolic process	105	1,31	-0,88					

Fig. 4 Heatmap highlighting DEGs explained by the interaction between infection and time of the day as detected in infected A .thaliana roots 14 DAI The row-normalised and log transformed gene counts are shown for each sample separately. The status of each sample is described by a combination of green (control plant) or purple (infected plant) and yellow (day) or (blue) bars. DEGs with similar patterns of expression have been grouped in 8 clusters (numbers in white boxes).

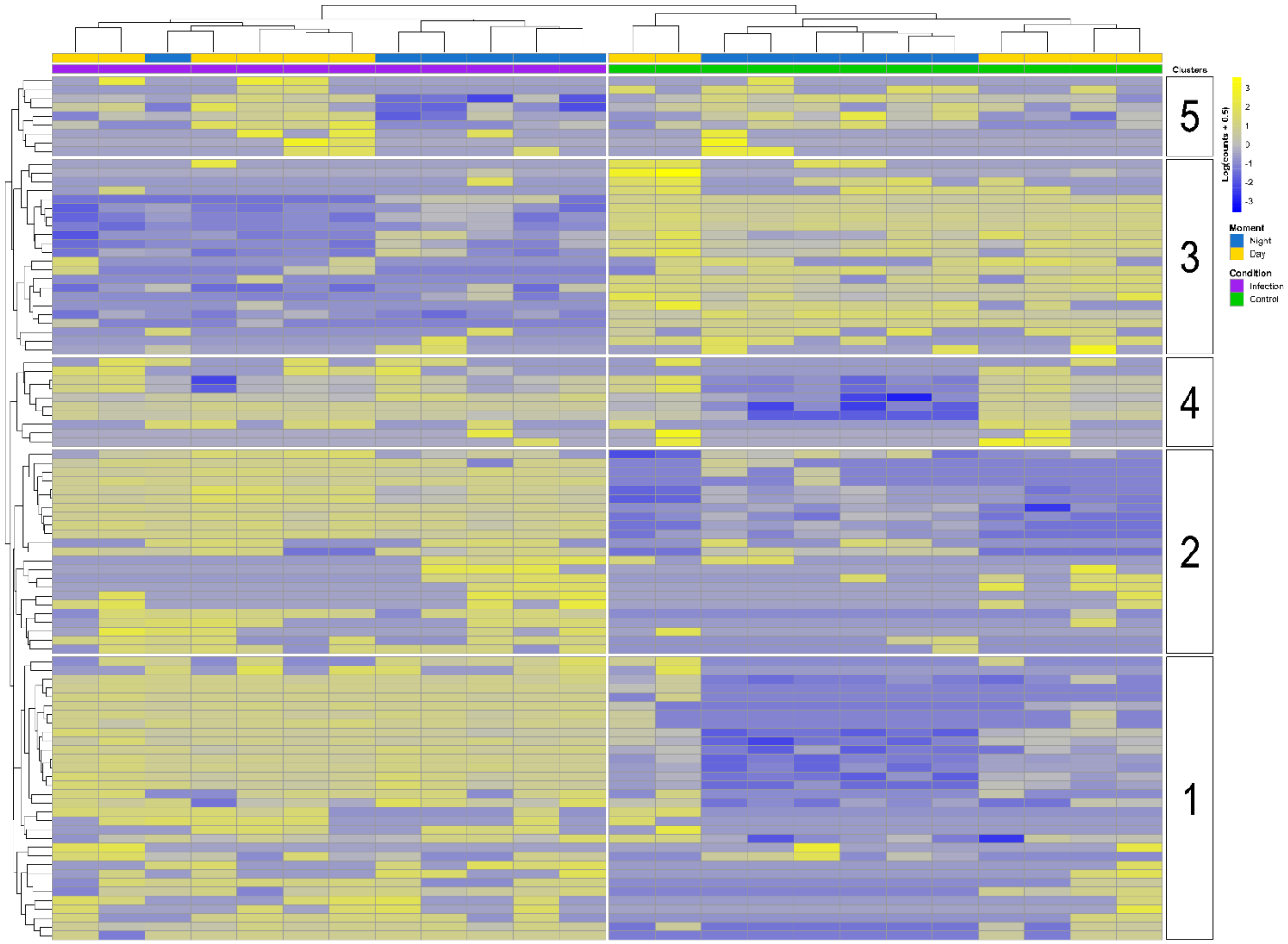

Fig. 5: Heatmap highlighting DEGs explained by the interaction between infection and time of the day as detected in infected A .thaliana roots 21 DAI The row-normalised and log transformed gene counts are shown for each sample separately. The status of each sample is described by a combination of green (control plant) or purple (infected plant) and yellow (day) or (blue) bars. DEGs with similar patterns of expression have been grouped in 5 clusters (numbers in white boxes).

Bibliography

[1] G. R. Dixon, “The occurrence and economic impact of plasmodiophora brassicae and clubroot disease,” *J. Plant Growth Regul.*, vol. 28, no. 3, pp. 194–202, 2009, doi: 10.1007/s00344-009-9090-y.

[2] R. Sierra *et al.*, “Evolutionary origins of rhizarian parasites,” *Mol. Biol. Evol.*, vol. 33, no. 4, pp. 980–983, 2016, doi: 10.1093/molbev/msv340.

[3] L. Liu, L. Qin, Z. Zhou, W. G. H. M. Hendriks, S. Liu, and Y. Wei, “Refining the life cycle of Plasmodiophora brassicae,” *Phytopathology*, vol. 110, no. 10, pp. 1704–1712, 2020, doi: 10.1094/PHYTO-02-20-0029-R.

[4] K. Kageyama and T. Asano, “Life cycle of plasmodiophora brassicae,” *J. Plant Growth Regul.*, vol. 28, no. 3, pp. 203–211, 2009, doi: 10.1007/s00344-009-9101-z.

[5] M. Olszak *et al.*, “Transcriptional profiling identifies critical steps of cell cycle reprogramming necessary for Plasmodiophora brassicae-driven gall formation in Arabidopsis,” *Plant J.*, vol. 97, no. 4, pp. 715–729, 2019, doi: 10.1111/tpj.14156.

[6] R. Malinowski, W. Truman, and S. Blicharz, “Genius architect or clever thief — How Plasmodiophora brassicae reprograms host development to establish a pathogen-oriented physiological sink,” *Mol. Plant-Microbe Interact.*, vol. 32, no. 10, pp. 1259–1266, 2019, doi: 10.1094/MPMI-03-19-0069-CR.

[7] M. A. Javed *et al.*, “The clubroot pathogen Plasmodiophora brassicae: A profile update,” *Mol. Plant Pathol.*, vol. 24, no. 2, pp. 89–106, 2023, doi: 10.1111/mpp.13283.

[8] J. Siemens *et al.*, “Transcriptome analysis of Arabidopsis clubroots indicate a key role for cytokinins in disease development,” *Mol. Plant-Microbe Interact.*, vol. 19, no. 5, pp. 480–494, 2006, doi: 10.1094/MPMI-19-0480.

[9] A. Agarwal, V. Kaul, R. Faggian, J. E. Rookes, J. Ludwig-Müller, and D. M. Cahill, “Analysis of global host gene expression during the primary phase of the Arabidopsis thalianaPlasmodiophora brassicae interaction,” *Funct. Plant Biol.*, vol. 38, no. 6, pp. 462–478, 2011, doi: 10.1071/FP11026.

[10] S. Irani *et al.*, “Transcriptome analysis of response to Plasmodiophora brassicae infection in the Arabidopsis shoot and root,” *BMC Genomics*, vol. 19, no. 1, p. 23, 2018, doi: 10.1186/s12864-017-4426-7.

[11] S. Ciaghi, A. Schwelm, and S. Neuhauser, “Transcriptomic response in symptomless roots of clubroot infected kohlrabi (Brassica oleracea var. gongylodes) mirrors resistant plants,” *BMC Plant Biol.*, vol. 19, no. 1, pp. 1–14, 2019, doi: 10.1186/s12870-019-1902-z.

[12] K. Stefanowicz *et al.*, “Plasmodiophora brassicae-Triggered Cell Enlargement and Loss of Cellular Integrity in Root Systems Are Mediated by Pectin Demethylation,” *Front. Plant Sci.*, vol. 12, no. July, 2021, doi: 10.3389/fpls.2021.711838.

[13] J. Tu, L. Qin, C. Karunakaran, Y. Wei, and G. Peng, “Lignin accumulation in cell wall plays a role in clubroot resistance,” *Front. Plant Sci.*, vol. 15, no. July, pp. 1–16, 2024, doi: 10.3389/fpls.2024.1401265.

[14] J. Siemens *et al.*, “Extracellular invertase is involved in the regulation of clubroot disease in

587 Arabidopsis thaliana," *Mol. Plant Pathol.*, vol. 12, no. 3, pp. 247–262, 2011, doi: 10.1111/j.1364-
588 3703.2010.00667.x.

589 [15] P. Walerowski *et al.*, "Clubroot disease stimulates early steps of phloem differentiation and
590 recruits SWEET sucrose transporters within developing galls," *Plant Cell*, vol. 30, no. 12, pp. 3058–
591 3073, 2018, doi: 10.1105/tpc.18.00283.

592 [16] J. Ludwig-Müller, E. Prinsen, S. A. Rolfe, and J. D. Scholes, "Metabolism and plant hormone action
593 during clubroot disease," *J. Plant Growth Regul.*, vol. 28, no. 3, pp. 229–244, 2009, doi:
594 10.1007/s00344-009-9089-4.

595 [17] S. Devos *et al.*, "A hormone and proteome approach to picturing the initial metabolic events
596 during Plasmodiophora brassicae infection on Arabidopsis," *Mol. Plant-Microbe Interact.*, vol. 19,
597 no. 12, pp. 1431–1443, 2006, doi: 10.1094/MPMI-19-1431.

598 [18] D. A. Lovelock *et al.*, "Analysis of salicylic acid-dependent pathways in Arabidopsis thaliana
599 following infection with Plasmodiophora brassicae and the influence of salicylic acid on disease,"
600 *Mol. Plant Pathol.*, vol. 17, no. 8, pp. 1237–1251, 2016, doi: 10.1111/mpp.12361.

601 [19] D. A. Lovelock, C. E. Donald, X. A. Conlan, and D. M. Cahill, "Salicylic acid suppression of clubroot
602 in broccoli (Brassicae oleracea var. italica) caused by the obligate biotroph Plasmodiophora
603 brassicae," *Australas. Plant Pathol.*, vol. 42, no. 2, pp. 141–153, 2013, doi: 10.1007/s13313-012-
604 0167-x.

605 [20] S. Lemarié *et al.*, "Both the Jasmonic Acid and the Salicylic Acid Pathways Contribute to Resistance
606 to the Biotrophic Clubroot Agent Plasmodiophora brassicae in Arabidopsis," *Plant Cell Physiol.*,
607 vol. 56, no. 11, pp. 2158–2168, 2015, doi: 10.1093/pcp/pcv127.

608 [21] A. Gravot *et al.*, "Arginase induction represses gall development during clubroot infection in
609 arabidopsis," *Plant Cell Physiol.*, vol. 53, no. 5, pp. 901–911, 2012, doi: 10.1093/pcp/pcs037.

610 [22] J. Ludwig-Müller *et al.*, "A novel methyltransferase from the intracellular pathogen
611 Plasmodiophora brassicae methylates salicylic acid," *Mol. Plant Pathol.*, vol. 16, no. 4, pp. 349–
612 364, 2015, doi: 10.1111/mpp.12185.

613 [23] A. Smolko *et al.*, "The GH3 Protein from the Clubroot Pathogen Plasmodiophora brassicae Causes
614 Hormone-Related Phenotypes in Arabidopsis thaliana," *J. Plant Growth Regul.*, vol. 43, no. 8, pp.
615 2715–2738, 2024, doi: 10.1007/s00344-024-11300-3.

616 [24] F. Vandenbussche *et al.*, "The Arabidopsis mutant alh1 illustrates a cross talk between ethylene
617 and auxin," *Plant Physiol.*, vol. 131, no. 3, pp. 1228–1238, 2003, doi: 10.1104/pp.010850.

618 [25] S. Grsic-Rausch, P. Kobelt, J. M. Siemens, M. Bischoff, and J. Ludwig-Müller, "Expression and
619 localization of nitrilase during symptom development of the clubroot disease in Arabidopsis,"
620 *Plant Physiol.*, vol. 122, no. 2, pp. 369–378, 2000, doi: 10.1104/pp.122.2.369.

621 [26] K. Neuhaus, S. Grsic-Rausch, S. Sauerteig, and J. Ludwig-Müller, "Arabidopsis plants transformed
622 with nitrilase 1 or 2 in antisense direction are delayed in clubroot development," *J. Plant Physiol.*,
623 vol. 156, no. 5–6, pp. 756–761, 2000, doi: 10.1016/S0176-1617(00)80243-6.

624 [27] A. Hurný *et al.*, "SYNERGISTIC ON AUXIN AND CYTOKININ 1 positively regulates growth and
625 attenuates soil pathogen resistance," *Nat. Commun.*, vol. 11, no. 1, 2020, doi: 10.1038/s41467-
626 020-15895-5.

[28] D. R. Walters and N. McRoberts, “Plants and biotrophs: a pivotal role for cytokinins?,” *Trends Plant Sci.*, vol. 11, no. 12, pp. 581–586, 2006, doi: 10.1016/j.tplants.2006.10.003.

[29] H. M. Dekhuijzen, “The Occurrence of Free and Bound Cytokinins in Plasmodia of Plasmodiophora brassicae Isolated from Tissue Cultures of Clubroots,” *Plant Cell Rep.*, vol. 213, pp. 29–30, 1981.

[30] H. M. Dekhuijzen and J. C. Overeem, “The role of cytokinins in clubroot formation,” *Physiol. Plant Pathol.*, vol. 1, no. 2, pp. 151–161, 1971, doi: 10.1016/0048-4059(71)90024-5.

[31] R. Malinowski, O. Novák, M. H. Borhan, L. Spíchal, M. Strnad, and S. A. Rolfe, “The role of cytokinins in clubroot disease,” *Eur. J. Plant Pathol.*, vol. 145, no. 3, pp. 543–557, 2016, doi: 10.1007/s10658-015-0845-y.

[32] S. A. Rolfe *et al.*, “The compact genome of the plant pathogen Plasmodiophora brassicae is adapted to intracellular interactions with host Brassica spp,” *BMC Genomics*, vol. 17, no. 1, pp. 1–15, 2016, doi: 10.1186/s12864-016-2597-2.

[33] P. Müller and W. Hilgenberg, “Isomers of zeatin and zeatin riboside in clubroot tissue: evidence for trans-zeatin biosynthesis by Plasmodiophora brassicae,” *Physiol. Plant.*, vol. 66, no. 2, pp. 245–250, 1986, doi: 10.1111/j.1399-3054.1986.tb02415.x.

[34] S. Devos, K. Vissenberg, J. P. Verbelen, and E. Prinsen, “Infection of Chinese cabbage by Plasmodiophora brassicae leads to a stimulation of plant growth: Impacts on cell wall metabolism and hormone balance,” *New Phytol.*, vol. 166, no. 1, pp. 241–250, 2005, doi: 10.1111/j.1469-8137.2004.01304.x.

[35] R. Henriques, C. Papdi, Z. Ahmad, and L. Bögre, “Circadian Regulation of Plant Growth,” *Annu. Plant Rev. online*, vol. 1, pp. 675–704, 2018, doi: 10.1002/9781119312994.apr0655.

[36] S. E. Sanchez and S. A. Kay, “The plant circadian clock: From a simple timekeeper to a complex developmental manager,” *Cold Spring Harb. Perspect. Biol.*, vol. 8, no. 12, pp. 1–16, 2016, doi: 10.1101/cshperspect.a027748.

[37] S. Wang, G. Steed, and A. A. R. Webb, “Circadian entrainment in Arabidopsis,” *Plant Physiol.*, vol. 190, no. 2, pp. 981–993, 2022, doi: 10.1093/plphys/kiac204.

[38] A. Graf, A. Schlereth, M. Stitt, and A. M. Smith, “Circadian control of carbohydrate availability for growth in Arabidopsis plants at night,” *Proc. Natl. Acad. Sci. U. S. A.*, vol. 107, no. 20, pp. 9458–9463, 2010, doi: 10.1073/pnas.0914299107.

[39] S. Mora-García, M. J. de Leone, and M. Yanovsky, “Time to grow: circadian regulation of growth and metabolism in photosynthetic organisms,” *Curr. Opin. Plant Biol.*, vol. 35, pp. 84–90, 2017, doi: 10.1016/j.pbi.2016.11.009.

[40] N. Yazdanbakhsh, R. Sulpice, A. Graf, M. Stitt, and J. Fisahn, “Circadian control of root elongation and C partitioning in Arabidopsis thaliana,” *Plant, Cell Environ.*, vol. 34, no. 6, pp. 877–894, 2011, doi: 10.1111/j.1365-3040.2011.02286.x.

[41] N. Yazdanbakhsh and J. Fisahn, “Analysis of Arabidopsis thaliana root growth kinetics with high temporal and spatial resolution.,” *Ann. Bot.*, vol. 105, no. 5, pp. 783–791, 2010, doi: 10.1093/aob/mcq048.

[42] M. Durand, D. Mainson, B. Porcheron, L. Maurousset, R. Lemoine, and N. Pourtau, “Carbon source–sink relationship in Arabidopsis thaliana: the role of sucrose transporters,” *Planta*, vol.

667 247, no. 3, pp. 587–611, 2018, doi: 10.1007/s00425-017-2807-4.

668 [43] D. Goodspeed, E. W. Chehab, A. Min-Venditti, J. Braam, and M. F. Covington, "Arabidopsis
669 synchronizes jasmonate-mediated defense with insect circadian behavior," *Proc. Natl. Acad. Sci.*
670 *U. S. A.*, vol. 109, no. 12, pp. 4674–4677, 2012, doi: 10.1073/pnas.1116368109.

671 [44] H. Lu, C. R. McClung, and C. Zhang, "Tick Tock: Circadian Regulation of Plant Innate Immunity,"
672 *Annu. Rev. Phytopathol.*, vol. 55, pp. 287–311, 2017, doi: 10.1146/annurev-phyto-080516-
673 035451.

674 [45] A. Schwelm *et al.*, "The Plasmodiophora brassicae genome reveals insights in its life cycle and
675 ancestry of chitin synthases," *Sci. Rep.*, vol. 5, no. May, pp. 1–12, 2015, doi: 10.1038/srep11153.

676 [46] M. Fähling, H. Graf, and J. Siemens, "Characterization of a Single-Spore Isolate Population of
677 Plasmodiophora brassicae Resulting from a Single Club," *J. Phytopathol.*, vol. 152, pp. 438–444,
678 2004.

679 [47] S. Andrews, "FastQC A Quality Control tool for High Throughput Sequence Data,"
680 http://www.bioinformatics.babraham.ac.uk/projects/fastqc/.

681 [48] P. Ewels, M. Magnusson, S. Lundin, and M. Käller, "MultiQC: Summarize analysis results for
682 multiple tools and samples in a single report," *Bioinformatics*, vol. 32, no. 19, pp. 3047–3048,
683 2016, doi: 10.1093/bioinformatics/btw354.

684 [49] B. Langmead and S. L. Salzberg, "Fast gapped-read alignment with Bowtie 2.," *Nat. Methods*, vol.
685 9, no. 4, pp. 357–9, 2012, doi: 10.1038/nmeth.1923.

686 [50] P. Lamesch *et al.*, "The Arabidopsis Information Resource (TAIR): Improved gene annotation and
687 new tools," *Nucleic Acids Res.*, vol. 40, no. D1, pp. 1202–1210, 2011, doi: 10.1093/nar/gkr1090.

688 [51] K. R. O'Keeffe and C. D. Jones, "Challenges and solutions for analysing dual RNA-seq data for non-
689 model host–pathogen systems," *Methods Ecol. Evol.*, vol. 10, no. 3, pp. 401–414, 2019, doi:
690 10.1111/2041-210X.13135.

691 [52] M. G. Grabherr *et al.*, "Full-length transcriptome assembly from RNA-Seq data without a
692 reference genome," *Nat. Biotechnol.*, vol. 29, no. 7, pp. 644–652, 2011, doi: 10.1038/nbt.1883.

693 [53] D. M. Bryant *et al.*, "A Tissue-Mapped Axolotl De Novo Transcriptome Enables Identification of
694 Limb Regeneration Factors," *Cell Rep.*, vol. 18, no. 3, pp. 762–776, 2017, doi:
695 10.1016/j.celrep.2016.12.063.

696 [54] A. Dobin *et al.*, "STAR: Ultrafast universal RNA-seq aligner," *Bioinformatics*, vol. 29, no. 1, pp. 15–
697 21, 2013, doi: 10.1093/bioinformatics/bts635.

698 [55] R. Patro, G. Duggal, M. I. Love, R. A. Irizarry, and C. Kingsford, "Salmon provides fast and bias-
699 aware quantification of transcript expression," *Nat. Methods*, vol. 14, no. 4, pp. 417–419, 2017,
700 doi: 10.1038/nmeth.4197.

701 [56] M. I. Love, W. Huber, and S. Anders, "Moderated estimation of fold change and dispersion for
702 RNA-seq data with DESeq2," *Genome Biol.*, vol. 15, no. 12, pp. 1–21, 2014, doi: 10.1186/s13059-
703 014-0550-8.

704 [57] R Core Team, "R: A Language and Environment for Statistical Computing." Vienna, Austria, 2021.
705 [Online]. Available: https://www.r-project.org/

[58] H. Wickham, “ggplot2: Elegant Graphics for Data Analysis,” *J. Stat. Softw.*, vol. 1, no. 1, pp. 128–129, 2010, doi: 10.1002/wics.10.

[59] H. Chen, “VennDiagram: Generate High-Resolution Venn and Euler Plots.” 2022. [Online]. Available: https://cran.r-project.org/package=VennDiagram

[60] T. Wu *et al.*, “clusterProfiler 4.0: A universal enrichment tool for interpreting omics data,” *Innovation*, vol. 2, no. 3, p. 100141, 2021, doi: 10.1016/j.xinn.2021.100141.

[61] W. Walter, F. Sánchez-Cabo, and M. Ricote, “GOplot: An R package for visually combining expression data with functional analysis,” *Bioinformatics*, vol. 31, no. 17, pp. 2912–2914, 2015, doi: 10.1093/bioinformatics/btv300.

[62] R. Kolde, “pheatmap: Pretty Heatmaps.” 2019. [Online]. Available: https://cran.r-project.org/package=pheatmap

[63] Inkscape Project, “Inkscape.” Retrieved from https://inkscape.org, 2020. [Online]. Available: https://inkscape.org

[64] J. C. Duda, C. Drenda, H. Kästel, J. Rahnenführer, and F. Kappenberg, “Benefit of using interaction effects for the analysis of high-dimensional time-response or dose-response data for two-group comparisons,” *Sci. Rep.*, vol. 13, no. 1, pp. 1–12, 2023, doi: 10.1038/s41598-023-47057-0.

[65] L. Kunkel, “Tissue invasion by Plasmodiophora brassicae,” *J. Agric. Res.*, vol. 12, no. 543, pp. 543–572, 1918.

[66] A. Schuller, J. Kehr, and J. Ludwig-Müller, “Laser microdissection coupled to transcriptional profiling of arabidopsis roots inoculated by plasmodiophora brassicae indicates a role for brassinosteroids in clubroot formation,” *Plant Cell Physiol.*, vol. 55, no. 2, pp. 392–411, 2014, doi: 10.1093/pcp/pct174.

[67] Y. Song, Y. Jiang, B. Kuai, and L. Li, “Circadian clock-associated 1 inhibits leaf senescence in arabidopsis,” *Front. Plant Sci.*, vol. 9, no. March, pp. 1–9, 2018, doi: 10.3389/fpls.2018.00280.

[68] H. Kim and S. Hong, “Role of the circadian clock in fine-tuning the process of leaf senescence in plants,” *Transl. Med. Aging*, vol. 3, no. 2019, pp. 26–30, 2019, doi: 10.1016/j.tma.2018.12.001.

[69] J. Lee, M. H. Kang, J. Y. Kim, and P. O. Lim, “The Role of Light and Circadian Clock in Regulation of Leaf Senescence,” *Front. Plant Sci.*, vol. 12, no. April, 2021, doi: 10.3389/fpls.2021.669170.

[70] E. Bustillo-Avendaño, L. Serrano-Ron, and M. A. Moreno-Risueno, “The Root Clock as a Signal Integrator System: Ensuring Balance for Survival,” *Front. Plant Sci.*, vol. 13, no. May, 2022, doi: 10.3389/fpls.2022.886700.

[71] W. Davis, M. Endo, and J. C. W. Locke, “Spatially specific mechanisms and functions of the plant circadian clock,” *Plant Physiol.*, vol. 190, no. 2, pp. 938–951, 2022, doi: 10.1093/plphys/kiac236.

[72] P. Perez-Garcia, L. Serrano-Ron, and M. A. Moreno-Risueno, “The nature of the root clock at single cell resolution: Principles of communication and similarities with plant and animal pulsatile and circadian mechanisms,” *Curr. Opin. Cell Biol.*, vol. 77, p. 102102, 2022, doi: 10.1016/j.ceb.2022.102102.

[73] M. Mortada, L. Xiong, and P. Mas, “Dissecting the complexity of local and systemic circadian communication in plants,” *npj Biol. Timing Sleep*, vol. 1, no. 1, pp. 1–7, 2024, doi: 10.1038/s44323-024-00003-3.

746 [74] J. A. Siqueira, W. C. Otoni, and W. L. Araújo, “The hidden half comes into the spotlight: Peeking
747 inside the black box of root developmental phases,” *Plant Commun.*, vol. 3, no. 1, pp. 1–17, 2022,
748 doi: 10.1016/j.xplc.2021.100246.

749 [75] D. W. Meinke, J. M. Cherry, C. Dean, S. D. Rounsley, and M. Koornneef, “Arabidopsis thaliana: A
750 model plant for genome analysis,” *Science (80-.).*, vol. 282, no. 5389, 1998, doi:
751 10.1126/science.282.5389.662.

752 [76] A. Gravot *et al.*, “Hypoxia response in Arabidopsis roots infected by Plasmodiophora brassicae
753 supports the development of clubroot,” *BMC Plant Biol.*, vol. 16, no. 1, pp. 1–10, 2016, doi:
754 10.1186/s12870-016-0941-y.

755 [77] N. Q. Dong and H. X. Lin, “Contribution of phenylpropanoid metabolism to plant development and
756 plant–environment interactions,” *J. Integr. Plant Biol.*, vol. 63, no. 1, pp. 180–209, 2021, doi:
757 10.1111/jipb.13054.

758 [78] A. Barkan and I. Small, “Pentatricopeptide repeat proteins in plants,” *Annu. Rev. Plant Biol.*, vol.
759 65, pp. 415–442, 2014, doi: 10.1146/annurev-arplant-050213-040159.

760 [79] X. Wang, Y. An, P. Xu, and J. Xiao, “Functioning of PPR Proteins in Organelle RNA Metabolism and
761 Chloroplast Biogenesis,” *Front. Plant Sci.*, vol. 12, no. February, pp. 1–8, 2021, doi:
762 10.3389/fpls.2021.627501.

763 [80] Y. Ma *et al.*, “Starch content changes and metabolism-related gene regulation of Chinese cabbage
764 synergistically induced by Plasmodiophora brassicae infection,” *Hortic. Res.*, 2022.

765 [81] A. Garvetto *et al.*, “Phagocytosis underpins the biotrophic lifestyle of intracellular parasites in the
766 class Phytomyxea (Rhizaria),” *New Phytol.*, vol. 238, no. 5, pp. 2130–2143, 2023, doi:
767 10.1111/nph.18828.

768 [82] M. Liebers *et al.*, “Regulatory shifts in plastid transcription play a key role in morphological
769 conversions of plastids during plant development,” *Front. Plant Sci.*, vol. 8, 2017, doi:
770 10.3389/fpls.2017.00023.

771 [83] K. Enami, T. Ozawa, N. Motohashi, M. Nakamura, K. Tanaka, and M. Hanaoka, “Plastid-to-nucleus
772 retrograde signals are essential for the expression of nuclear starch biosynthesis genes during
773 amyloplast differentiation in tobacco BY-2 cultured cells,” *Plant Physiol.*, vol. 157, no. 1, pp. 518–
774 530, 2011, doi: 10.1104/pp.111.178897.

775 [84] Y. Miyazawa, A. Sakai, S. Y. Miyagishima, H. Takano, S. Kawano, and T. Kuroiwa, “Auxin and
776 cytokinin have opposite effects on amyloplast development and the expression of starch
777 synthesis genes in cultured Bright Yellow-2 tobacco cells,” *Plant Physiol.*, vol. 121, no. 2, pp. 461–
778 469, 1999, doi: 10.1104/pp.121.2.461.

779 [85] N. T. Keen and P. H. Williams, “Translocation of Sugars into Infected Cabbage Tissues during
780 Clubroot Development,” *Plant Physiol.*, vol. 44, no. 5, pp. 748–754, 1969.

781 [86] K. Kobayashi *et al.*, “Lovastatin insensitive 1, a novel pentatricopeptide repeat protein, is a
782 potential regulatory factor of isoprenoid biosynthesis in Arabidopsis,” *Plant Cell Physiol.*, vol. 48,
783 no. 2, pp. 322–331, 2007, doi: 10.1093/pcp/pcm005.

784 [87] Y. Yang *et al.*, “Cytidine-to-uridine RNA editing factor NbMORF8 negatively regulates plant
785 immunity to phytophthora pathogens,” *Plant Physiol.*, vol. 184, no. 4, pp. 2182–2198, 2020, doi:
786 10.1104/pp.20.00458.

[88] J. Y. Zhu, E. Oh, T. Wang, and Z. Y. Wang, “TOC1-PIF4 interaction mediates the circadian gating of thermoresponsive growth in Arabidopsis,” *Nat. Commun.*, vol. 7, pp. 1–10, 2016, doi: 10.1038/ncomms13692.

[89] S. Kidokoro *et al.*, “Clock-regulated coactivators selectively control gene expression in response to different temperature stress conditions in Arabidopsis,” *Proc. Natl. Acad. Sci.*, vol. 120, no. 16, pp. 1–11, 2023, doi: 10.1073/pnas.

[90] X. Wei *et al.*, “Root Transcriptome and Metabolome Profiling Reveal Key Phytohormone-Related Genes and Pathways Involved Clubroot Resistance in Brassica rapa L.,” *Front. Plant Sci.*, vol. 12, no. December, pp. 1–17, 2021, doi: 10.3389/fpls.2021.759623.

[91] C. P. A. Jayasinghege, J. A. Ozga, V. P. Manolii, S. F. Hwang, and S. E. Strelkov, “Impact of Susceptibility on Plant Hormonal Composition during Clubroot Disease Development in Canola (Brassica napus),” *Plants*, vol. 12, no. 16, 2023, doi: 10.3390/plants12162899.

[92] E. M. Farré and T. Liu, “The PRR family of transcriptional regulators reflects the complexity and evolution of plant circadian clocks,” *Curr. Opin. Plant Biol.*, vol. 16, no. 5, pp. 621–629, 2013, doi: 10.1016/j.pbi.2013.06.015.

[93] A. Para, E. M. Farré, T. Imaizumi, J. L. Pruneda-Paz, F. G. Harmon, and S. A. Kay, “PRR3 is a vascular regulator of TOC1 stability in the Arabidopsis circadian clock,” *Plant Cell*, vol. 19, no. 11, pp. 3462–3473, 2007, doi: 10.1105/tpc.107.054775.

[94] A. Frank *et al.*, “Circadian Entrainment in Arabidopsis by the Sugar-Responsive Transcription Factor bZIP63,” *Curr. Biol.*, vol. 28, no. 16, pp. 2597-2606.e6, 2018, doi: 10.1016/j.cub.2018.05.092.

[95] W. Chen *et al.*, “SnRK1.1-mediated resistance of Arabidopsis thaliana to clubroot disease is inhibited by the novel Plasmodiophora brassicae effector PBZF1,” *Mol. Plant Pathol.*, vol. 22, no. 9, pp. 1057–1069, 2021, doi: 10.1111/mpp.13095.

[96] C. Han, H. Wang, W. Shi, and M.-Y. Bai, “The molecular associations between the SnRK1 complex and carbon/nitrogen metabolism in plants,” *New Crop.*, vol. 1, no. December 2023, p. 100008, 2024, doi: 10.1016/j.ncrops.2023.12.003.

[97] K. Uemoto *et al.*, “Root PRR7 Improves the Accuracy of the Shoot Circadian Clock through Nutrient Transport,” *Plant Cell Physiol.*, vol. 64, no. 3, pp. 352–362, 2023, doi: 10.1093/pcp/pcad003.

[98] M. Seki *et al.*, “Adjustment of the Arabidopsis circadian oscillator by sugar signalling dictates the regulation of starch metabolism,” *Sci. Rep.*, vol. 7, no. 1, pp. 1–11, 2017, doi: 10.1038/s41598-017-08325-y.

[99] M. J. Haydon, O. Mielczarek, A. Frank, Á. Román, and A. A. R. Webb, “Sucrose and ethylene signaling interact to modulate the circadian clock,” *Plant Physiol.*, vol. 175, no. 2, pp. 947–958, 2017, doi: 10.1104/pp.17.00592.

[100] N. Dalchau *et al.*, “The circadian oscillator gene GIGANTEA mediates a long-term response of the Arabidopsis thaliana circadian clock to sucrose,” *Proc. Natl. Acad. Sci. U. S. A.*, vol. 108, no. 12, pp. 5104–5109, 2011, doi: 10.1073/pnas.1015452108.

[101] E. Shor, I. Paik, S. Kangisser, R. Green, and E. Huq, “PHYTOCHROME INTERACTING FACTORS mediate metabolic control of the circadian system in Arabidopsis,” *New Phytol.*, vol. 215, no. 1,

pp. 217–228, 2017, doi: 10.1111/nph.14579.

[102] M. A. Nohales *et al.*, “Multi-level Modulation of Light Signaling by GIGANTEA Regulates Both the Output and Pace of the Circadian Clock,” *Dev. Cell*, vol. 49, no. 6, pp. 840-851.e8, 2019, doi: 10.1016/j.devcel.2019.04.030.

[103] Y. J. Park, J. Y. Kim, J. H. Lee, B. D. Lee, N. C. Paek, and C. M. Park, “GIGANTEA Shapes the Photoperiodic Rhythms of Thermomorphogenic Growth in Arabidopsis,” *Mol. Plant*, vol. 13, no. 3, pp. 459–470, 2020, doi: 10.1016/j.molp.2020.01.003.

[104] M. Thiruvengadam, C. F. Shih, and C. H. Yang, “Expression of An Antisense Brassica oleracea GIGANTEA (BoGI) Gene in Transgenic Broccoli Causes Delayed Flowering, Leaf Senescence, and Post-Harvest Yellowing Retardation,” *Plant Mol. Biol. Report.*, vol. 33, no. 5, pp. 1499–1509, 2015, doi: 10.1007/s11105-015-0852-3.

[105] M. A. Nohales and S. A. Kay, “GIGANTEA gates gibberellin signaling through stabilization of the DELLA proteins in Arabidopsis,” *Proc. Natl. Acad. Sci. U. S. A.*, vol. 116, no. 43, pp. 21893–21899, 2019, doi: 10.1073/pnas.1913532116.

[106] M. Shtin, R. Dello Ioio, and M. Del Bianco, “It’s Time for a Change: The Role of Gibberellin in Root Meristem Development,” *Front. Plant Sci.*, vol. 13, no. May, pp. 1–7, 2022, doi: 10.3389/fpls.2022.882517.

Additional Files

Additional File 1 Detailed overview of the samples sequenced in this study

Condition	Age (days after infection)	Hours after artificial dawn	Sample code	Raw reads
Control	14	5 hr 50' (day)	127925	41193025
		5 hr 50' (day)	127935	50545664
		5 hr 50' (day)	127936	35205326
		10 hr 40' (day)	127906	56725609
		10 hr 40' (day)	127912	54273366
		10 hr 40' (day)	127918	38720139
		15 hr 30' (night)	127926	41309013
		15 hr 30' (night)	127931	55027843
		15 hr 30' (night)	127937	38004169
		19 hr 20' (night)	127907	39958547
		19 hr 20' (night)	127913	37101449
		19 hr 20' (night)	127919	40693049
Infected	14	5 hr 50' (day)	127964	48508205
		5 hr 50' (day)	127970	41810661
		5 hr 50' (day)	127976	54739923
		10 hr 40' (day)	127946	42594195
		10 hr 40' (day)	127952	41155738
		10 hr 40' (day)	127958	58101982
		15 hr 30' (night)	127965	43247574
		15 hr 30' (night)	127971	46509846
		15 hr 30' (night)	127977	57602784
		19 hr 20' (night)	127947	40263406
		19 hr 20' (night)	127953	41398461
		19 hr 20' (night)	127959	50627500
Control	21	5 hr 50' (day)	127908	52533389
		5 hr 50' (day)	127914	36118824
		5 hr 50' (day)	127941	64871718
		10 hr 40' (day)	127928	41179331
		10 hr 40' (day)	127933	45662748
		10 hr 40' (day)	127939	54002775
		15 hr 30' (night)	127909	43278660
		15 hr 30' (night)	127915	43201375
		15 hr 30' (night)	127920	42466381
		19 hr 20' (night)	127929	43287455
		19 hr 20' (night)	127934	46270564
		19 hr 20' (night)	127940	53657896
Infected	21	5 hr 50' (day)	127948	59286277
		5 hr 50' (day)	127954	62740880
		5 hr 50' (day)	127960	46195940
		10 hr 40' (day)	127967	48074903

10 hr 40' (day)	127973	61491275
10 hr 40' (day)	127979	62580301
15 hr 30' (night)	127949	55537283
15 hr 30' (night)	127955	65514599
15 hr 30' (night)	127961	54889653
19 hr 20' (night)	127968	85469436
19 hr 20' (night)	127974	71731948
19 hr 20' (night)	127980	58536488

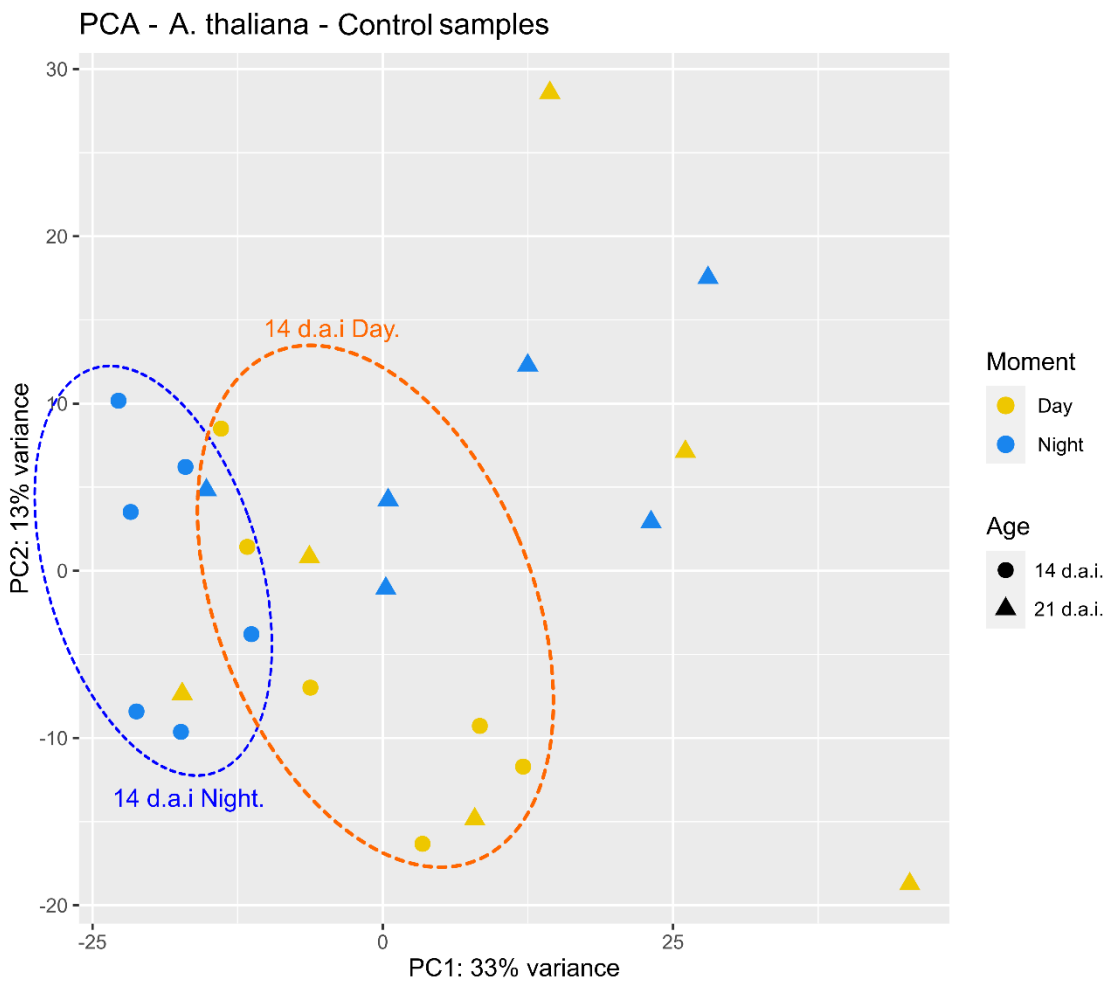

873

874 *Additional File 2 PCA on control A. thaliana plants, showing the decreased influence of the temporal factor (i.e., day and night)*
875 *on the overall gene expression levels with the ageing of the plants.*

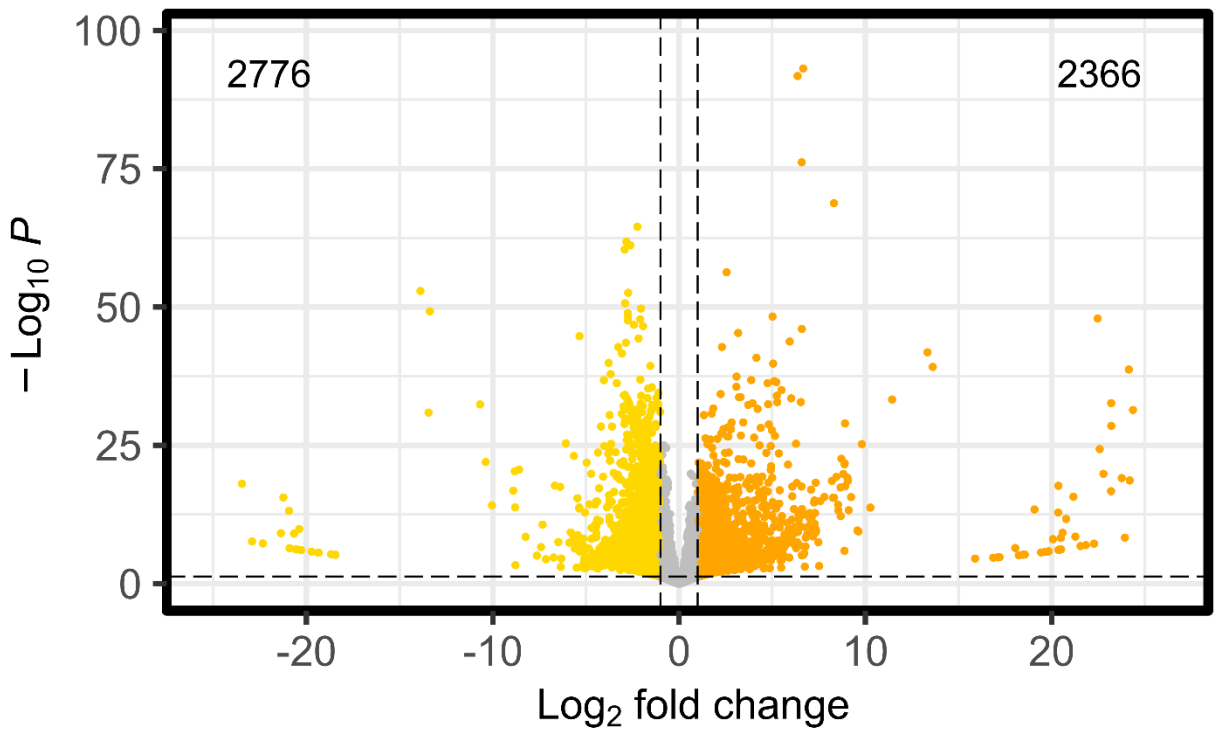

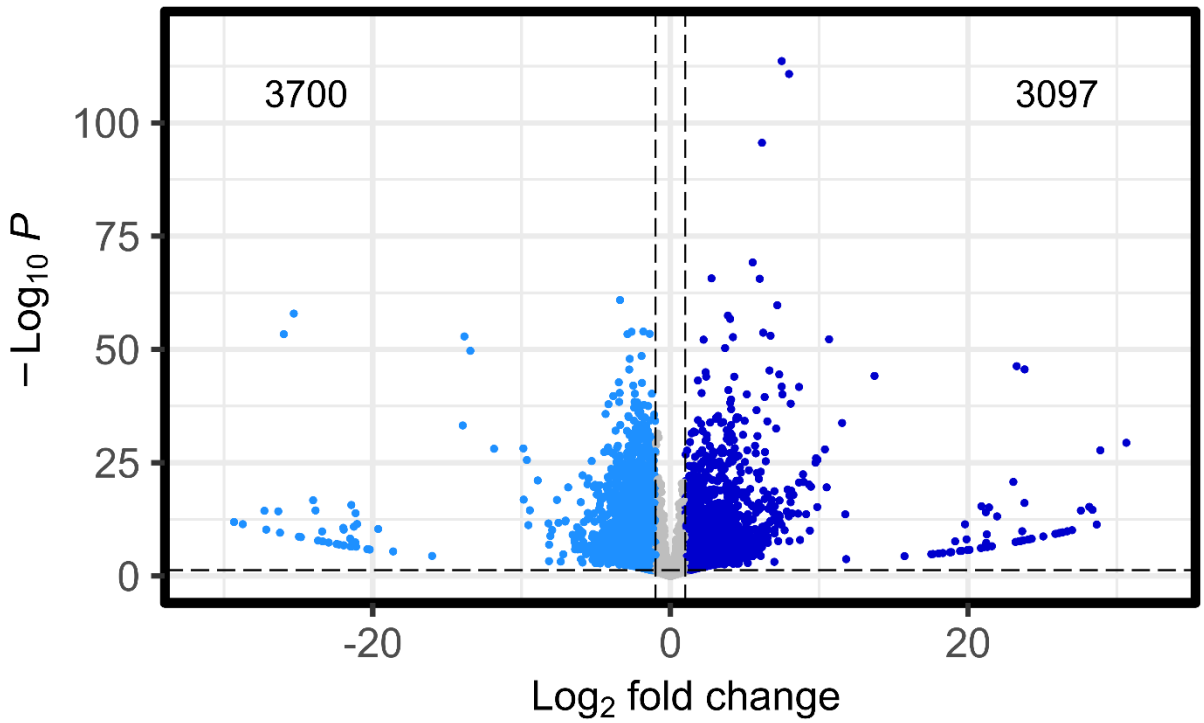

Additional File 3 Volcano plot showing the number of DEGs in the day (top figure) and night (bottom figure) in infected A. thaliana plants 14 DAI

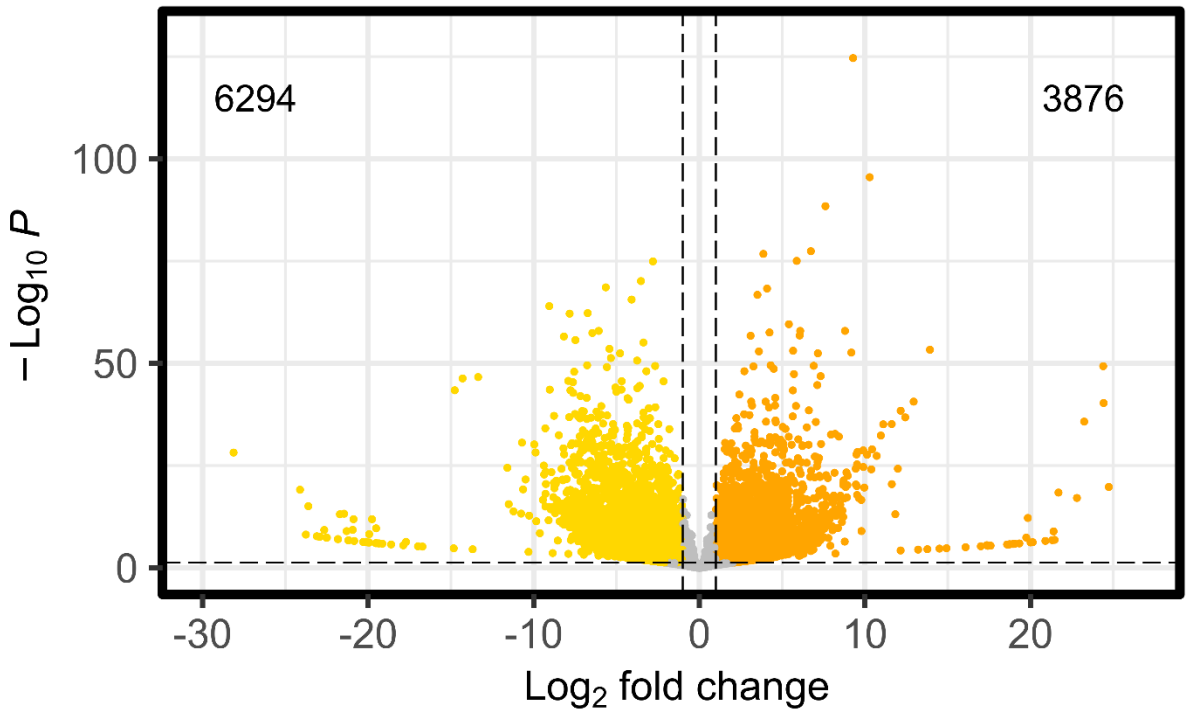

881

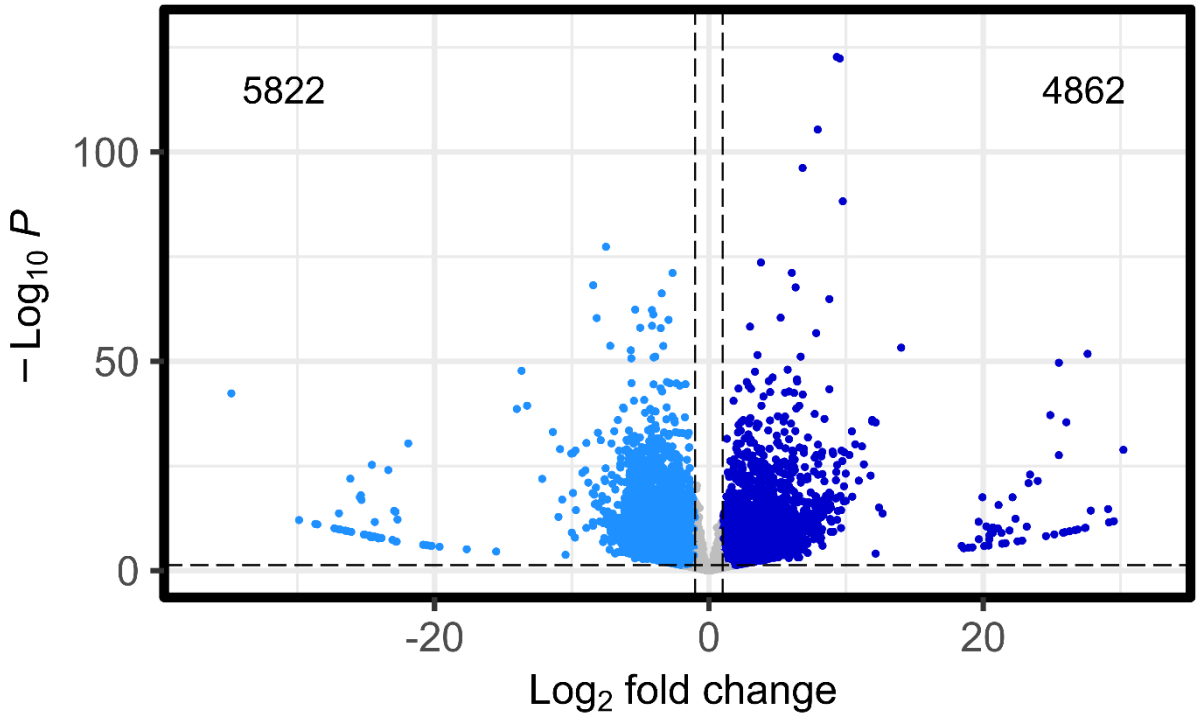

882

883 *Additional File 4 Volcano plot showing the number of DEGs in the day (top figure) and night (bottom figure) in infected A.*
884 *thaliana plants 21 DAI*

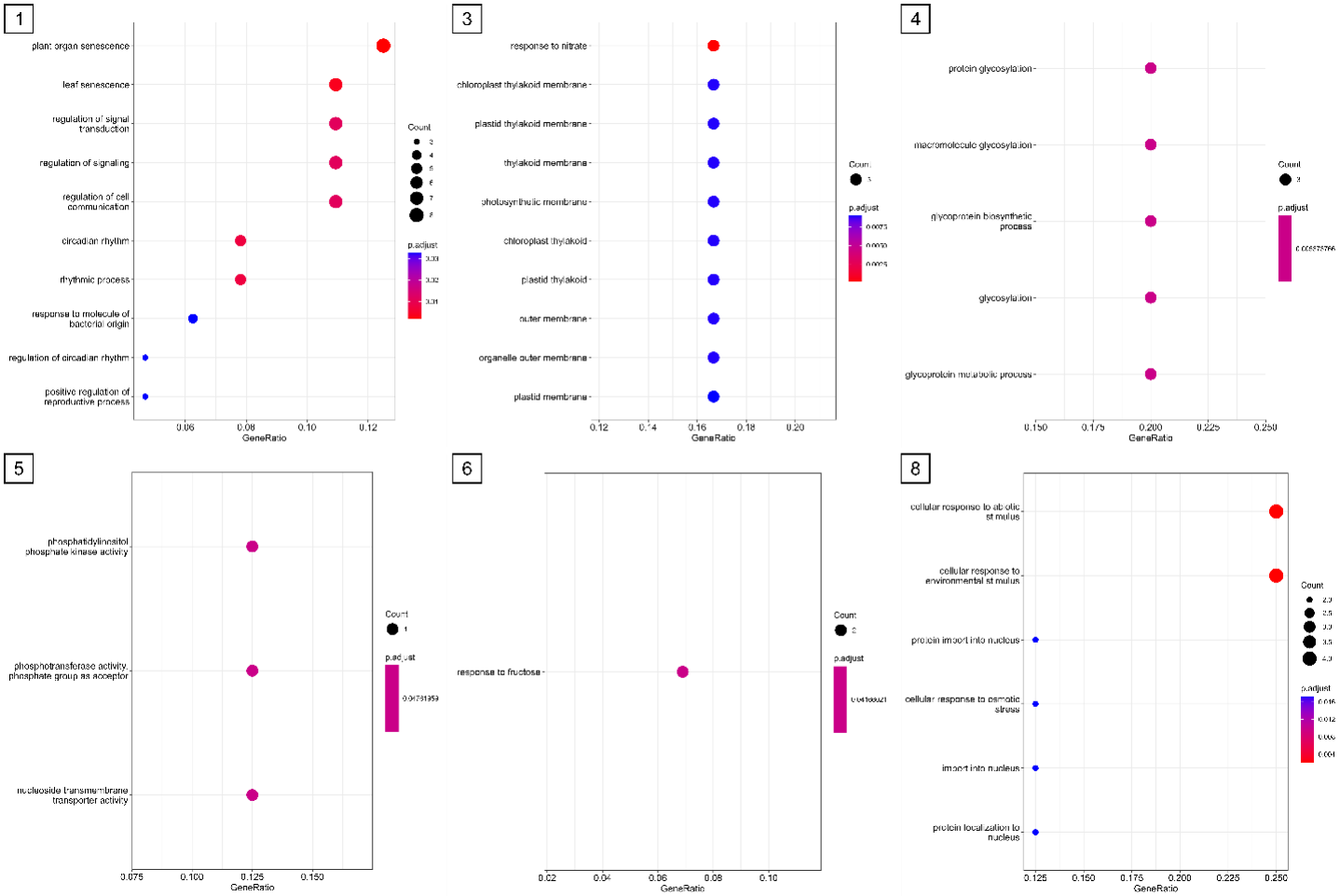

Additional File 5 GO terms overrepresentation analysis of the clusters of DEGs driven by the interaction between infection and time of the day 14 DAI

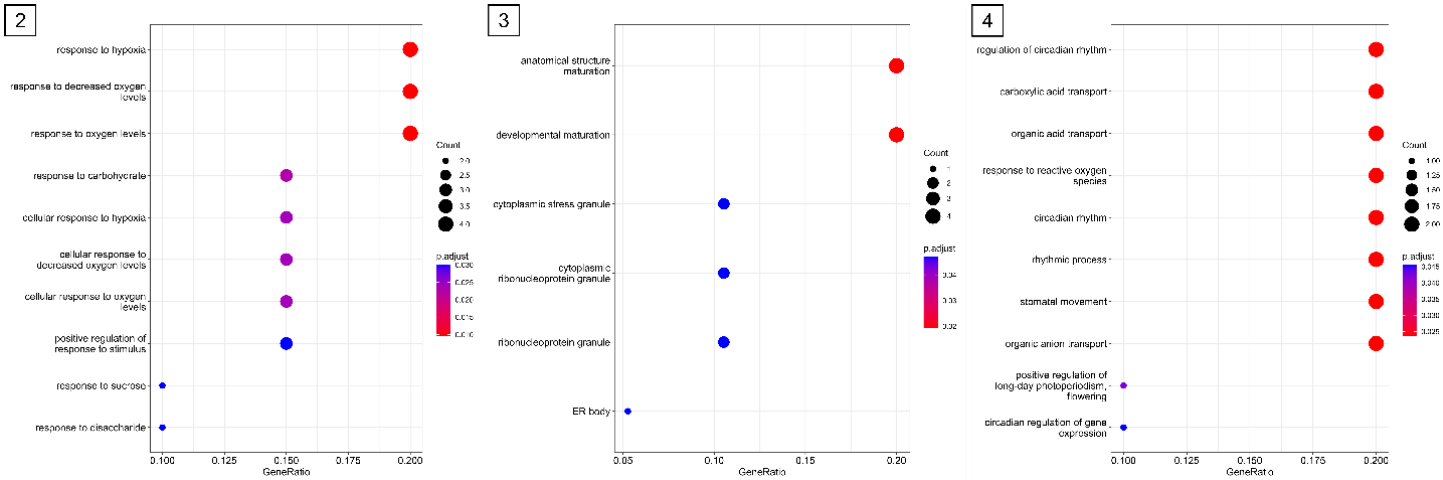

Additional File 6 GO terms overrepresentation analysis of the clusters of DEGs driven by the interaction between infection and time of the day 21 DAI